Adaptive Control of Body Posture and Movement in Quadruped Robots

Despina Ekaterini Argiropoulos

Thesis submitted in partial fulfillment of the requirements for the

Masters' of Science degree in Computer Science and Engineering

University of Crete
School of Sciences and Engineering
Computer Science Department
Voutes University Campus, 700 13 Heraklion, Crete, Greece

Thesis Advisor: Prof. *Panos Trahanias*

This work has been performed at the University of Crete, School of Sciences and Engineering, Computer Science Department.

The work has been supported by the Foundation for Research and Technology - Hellas (FORTH), Institute of Computer Science (ICS).

University of Crete
Computer Science Department

Adaptive Control of Body Posture and Movement in Quadruped Robots

Thesis submitted by
Despina Ekaterini Argiropoulos
in partial fulfillment of the requirements for the
Masters' of Science degree in Computer Science

THESIS APPROVAL

Author: _____
Despina Ekaterini Argiropoulos

Committee approvals: _____
Panos Trahanias
Professor, Thesis Supervisor

_____
Dimitrios Papageorgiou
Assistant Professor, Committee Member

_____
Antonios Argyros
Professor, Committee Member

Departmental approval: _____
Polyvios Pratikakis
Associate Professor, Director of Graduate Studies

Heraklion, November 2023

Adaptive Control of Body Posture and Movement in Quadruped Robots

Abstract

One of the primary advantages of legged robots lies in their ability to navigate through complex and unstructured environments, such as outdoor fields, sewers and construction sites, which often feature a variety of challenging terrains. This capability opens the door to employing legged robots in applications that might pose risks to humans, including search and rescue missions, inspection tasks and maintenance in critical infrastructure facilities.

In addition to the structural intricacies of these environments, they also present dynamic challenges, with varying terrain friction being a prominent concern. Legged robots frequently encounter the issue of partially or globally slippery terrains, which can result from conditions like mud, wet surfaces, oil or ice. The slippage of any leg relative to the supporting surface can introduce unpredictable and unmodeled dynamics, potentially compromising trajectory tracking performance or even leading to the robot's instability from loss of contact with the supporting surface.

In such conditions, maintaining stability and precise control becomes paramount. Ensuring that the robot follows desired trajectories with accuracy is not only essential for its own safety but also critical for successfully executing dexterous maneuvers in these challenging settings. Task space trajectory tracking plays a central role in achieving these objectives, as it enables the robot to adapt to the dynamic nature of its surroundings, react to unanticipated disturbances, and minimize the risk of falls or instability. By focusing on accurate tracking of task space trajectories, we aim to equip quadruped robots with the capability to operate with confidence and reliability in the face of environmental uncertainties.

Driven by the challenges posed by agile maneuvers and locomotion in rough and slippery terrains, we introduce an adaptive controller termed as the Body Posture and Movement Controller (BPMC) designed specifically for such conditions. BPMC comprises two key components: an adaptive trajectory tracking controller, referred to as "Body Posture", and an adaptive reaching-target controller that initiates locomotion, called "Body Movement".

The former, namely Body Posture controller, comprises a robust adaptive trajectory tracking controller that consists of two prioritized layers of adaptation aimed at maintaining stability during dynamic contact events of one or more supporting legs. The main objective of the proposed adaptive controller is to induce a robust reactive behaviour of a quadruped robot when it experiences unstable contacts while executing a trajectory without sacrificing the spatial properties of the task.

The Body Movement controller, serving as an adaptive reaching controller, plays a pivotal role in initiating locomotion tasks and executing agile maneuvers, particularly in challenging terrains marked by slipperiness and dynamic obstacles. The core of the Body Movement controller lies in its initial layer, in which the

control effort is distributed among all stance legs, meaning all legs except the swinging leg. The latter is accomplished by assigning an exceptionally high weight to a specific leg, designated as the swinging leg. In that way, the swinging leg task is attained while, at the same time, the robot keeps its stability and controllability during locomotion.

On top of that, the Body Movement controller offers an additional layer that can be activated at the user's discretion, taking into account the probability of detecting slip events. This extra layer draws inspiration from the approach used in the first layer of the Body Posture controller. It dynamically adjusts the effort distribution among all legs based on the slip probability of each foot. This multifaceted approach not only introduces innovative concepts for agile movements but also ensures the stability of the robot's dynamic maneuvers. It represents a crucial step in advancing the adaptability and robustness of the overall system.

The proposed methods constitute novel, lightweight analytical solutions that assume no prior knowledge of the friction properties of the supporting surface. This is accomplished by considering the slippage probability as extracted by our previous work on contact state estimation in order to avoid non-controllable conditions.

Our experimental outcomes, stemming from both simulations and real-world tests, highlight the approach's effectiveness. It substantially enhances system robustness, minimizing leg slippage while maintaining robot stability and control even in challenging conditions. These advances mark significant milestones in enhancing quadruped robot capabilities for diverse real-world scenarios.

Προσαρμοστικός Έλεγχος Πόζας Σώματος και Κίνησης Τετράποδων Ρομπότ

Περίληψη

Ένα από τα κύρια πλεονεκτήματα των τετράποδων ρομποτικών συστημάτων είναι η δυνατότητά τους να πλοηγούνται σε πολύπλοκα και μη δομημένα περιβάλλοντα, όπως εξωτερικοί χώροι, αποχετευτικά δίκτυα και εργοτάξια, τα οποία συχνά περιλαμβάνουν εδάφη που είναι δύσκολα στην προσπέλαση. Αυτή η ικανότητα τους οδηγεί στη χρήση των τετράποδων ρομπότ σε εφαρμογές που χαρακτηρίζονται επικίνδυνες για τον άνθρωπο, συμπεριλαμβανομένων αποστολών έρευνας και διάσωσης και εργασιών ελέγχου και συντήρησης σε εγκαταστάσεις κρίσιμης υποδομής.

Εκτός από τις δομικές περιπλοκές αυτών των περιβάλλοντων, ενίοτε παρουσιάζουν και δυναμικές προκλήσεις, με τη μεταβλητή τριβή του εδάφους να αποτελεί ένα σημαντικό θέμα. Τα ρομπότ με πόδια συχνά αντιμετωπίζουν το πρόβλημα ολισθηρών εδαφών, που μπορεί να οφείλεται σε συνθήκες όπως λάσπη, υγρές επιφάνειες, λάδι ή πάγο. Η ολίσθηση ενός ποδιού σε σχέση με την επιφάνεια στήριξης μπορεί να επιφέρει δυναμικές που αφενός είναι απρόβλεπτες και αφετέρου δεν μπορούν να μοντελοποιηθούν. Τα παραπάνω μπορεί να οδηγήσουν στη μη ακριβή παρακολούθηση της τροχιάς κίνησης από το ρομποτικό σύστημα ή ακόμα και στην απώλεια ελέγχου του σε περίπτωση που χαθεί η επαφή κάποιων ποδιών του ρομπότ με την επιφάνεια στήριξης.

Σε τέτοιες συνθήκες, η διατήρηση της ευστάθειας και του ελέγχου του ρομπότ αποκτά πρωταρχική σημασία. Επιπρόσθετα, η εξασφάλιση της ακριβούς παρακολούθησης της ζητούμενης τροχιάς κίνησης παίζει σημαντικό ρόλο όχι μόνο στην επίτευξη επιδέξιων ελιγμών και χειρισμών αλλά και στην ασφάλεια του ίδιου του συστήματος. Κατά συνέπεια, με την βελτίωση των σχετικών μεθόδων που αποσκοπούν στην πιστή παρακολούθηση τροχιάς, το ρομποτικά συστήματα εξελίσουν τις δυνατότητες τους ως προς εργασίες που αφορούν δύσκολα περιβάλλοντα. Συγκεκριμένα, αναπτύσουν δυνατότητες που αφορούν την προσαρμογή τους σε δυναμικές αλλαγές του περιβάλλοντος, εξαλείφοντας απρόβλεπτες διαταραχές, ενώ την ίδια στιγμή ελαχιστοποιούνται περιπτώσεις έλειψης ελέγχου και αποφεύγονται ακόμα πιθανές πτώσεις του συστήματος. Διασφαλίζεται έτσι η ευστάθεια και η αξιοπιστία των ρομποτικών συστημάτων σε περιπτώσεις όπου υπάρχει μεγάλη αβεβαιότητα στο περιβάλλον.

Οι προκλήσεις που παρουσιάστηκαν παραπάνω σχετικά με την επίτευξη επιδέξιων ρομποτικών κινήσεων και βάδισης σε ανώμαλα και ολισθηρά εδάφη λειτούργησαν ως το έναυσμα της έρευνας στην παρούσα εργασία. Το σημαντικότερο αποτέλεσμα αυτής είναι ένας προσαρμοστικός ελεγκτής 'Πόζας Σώματος και Κίνησης' (BPMC). Ο τελευταίος αποτελείται από δύο κύρια μέρη: έναν προσαρμοστικό ελεγκτή παρακολούθησης τροχιάς, που αναφέρεται ως 'Πόζα Σώματος', και έναν προσαρμοστικό ελεγκτή προσέγγισης στόχου, που αναφέρεται ως 'Κίνηση Σώματος' και αφορά την βάδιση του ρομποτικού συστήματος.

Ο πρώτος, δηλαδή ο ελεγκτής 'Πόζας Σώματος', περιλαμβάνει έναν προσαρμοστικό ελεγκτή παρακολούθησης τροχιάς που αποτελείται από δύο επίπεδα προσαρμογής,

με στόχο τη διατήρηση της ευστάθειας και του ελέγχου κατά τη διάρκεια που ένα, παραπάνω ή και όλα τα πόδια του ρομποτικού συστήματος γλιστρήσουν. Ο κύριος στόχος του προτεινόμενου ελεγκτή είναι να προσδώσει συμπεριφορά αντίδρασης στο τετράποδο ρομπότ όταν αντιμετωπίζει ασταθείς επαφές κατά την εκτέλεση της παρακολούθησης τροχιάς, χωρίς να θυσιάσει τις χωρικές ιδιότητες της ζητούμενης εργασίας.

Ο ελεγκτής Κίνησης Σώματος, που αποτελεί έναν ελεγκτή προσέγγισης στόχου, εισάγει την βάδιση του τετράποδου ρομπότ ενώ την ίδια χρονική στιγμή έχει την δυνατότητα να εκτελέσει επιδέξιους ελιγμούς, ειδικά σε απαιτητικά εδάφη που χαρακτηρίζονται από ολισθηρότητα και δυναμικά εμπόδια.

Το βασικό επίπεδο του ελεγκτή Κίνησης Σώματος αφορά την κατανομή της απαιτούμενης δύναμης σε όλα τα πόδια τα οποία στηρίζουν το ρομπότ κατά τη διάρκεια της βάδισής του, δηλαδή όλα τα πόδια εκτός του ποδιού που βρίσκεται σε κίνηση τροχιάς (αιωρούμενο πόδι). Αυτό επιτυγχάνεται με την ανάθεση εξαιρετικά υψηλών τιμών βάρους σε ένα συγκεκριμένο πόδι, που στην συγκρκριμένη σχεδίαση αφορά το αιωρούμενο πόδι. Με αυτόν τον τρόπο, επιτυγχάνεται η εκτέλεση της εργασίας από το πόδι που κινείται, ενώ ταυτόχρονα το ρομπότ διατηρεί τη ευστάθεια του κατά τη διάρκεια της κίνησης.

Επιπλέον, ο ελεγκτής Κίνησης Σώματος προσφέρει ένα επιπρόσθετο επίπεδο που μπορεί να ενεργοποιηθεί κατόπιν επιλογής του χρήστη, λαμβάνοντας υπόψη την πιθανότητα ανίχνευσης γλιστρίματος μεταξύ κάποιου ποδιού και του εδάφους. Αυτό το επιπρόσθετο επίπεδο βασίζεται στην προσέγγιση που χρησιμοποιείται στο πρώτο επίπεδο του ελεγκτή Στάσης Σώματος. Προσαρμόζει ανάλογα την κατανομή της δύναμης μεταξύ όλων των ποδιών με βάση την πιθανότητα ολίσθησης κάθε ποδιού. Αυτή η πολυδιάστατη προσέγγιση δεν εισάγει μόνο καινοτόμες έννοιες για ευέλικτες κινήσεις, αλλά εξασφαλίζει επίσης την ευστάθεια των δυναμικών κινήσεων του ρομπότ. Αποτελεί έτσι ένα κρίσιμο βήμα για την προώθηση της προσαρμοστικότητας και της ανθεκτικότητας του συνολικού συστήματος.

Οι προτεινόμενες μέθοδοι αποτελούν καινοτόμες, χαμηλού υπολογιστικού κόστους αναλυτικές λύσεις που δεν βασίζονται σε προηγούμενη γνώση σχετικά με τις ιδιότητες τριβής της επιφάνειας στήριξης ούτε απαιτούν εκτίμηση αυτών. Αυτό επιτυγχάνεται λαμβάνοντας υπόψη την πιθανότητα ολίσθησης, όπως αυτή εξάγεται από προηγούμενη εργασία μας σχετικά με την εκτίμηση κατάστασης επαφής, προκειμένου να αποφευχθούν μη ελεγχόμενες καταστάσεις σε ολισθηρά εδάφη.

Η παρούσα εργασία υποστηρίζεται από ιδιαίτερα ενθαρρυντικά πειραματικά αποτελέσματα. Τα τελευταία προέρχονται τόσο από προσομοιώσεις όσο και από πειράματα σε πραγματικά ρομποτικά συστήματα και αναδεικνύουν την αποτελεσματικότητα της προτεινόμενης προσέγγισης. Πιο συγκεκριμένα, η αξιοπιστία της μεθόδου δοκιμάζεται και κατά την εκτέλεση παρακολούθησης τροχιάς καθώς και κατά την διάρκεια βάδισης σε δύσκολα εδάφη. Σε όλες τις πειραματικές δοκιμασίες παρατηρούμε ότι οι ελεγκτές προσαρμόζονται μειώνοντας σημαντικά την ολίσθηση των ποδιών, ενώ διατηρείται η ευστάθεια και ο έλεγχος του τετράποδου ρομπότ ακόμα και σε απαιτητικές συνθήκες. Τα παραπάνω αποτελέσματα αποτελούν σημαντικά ορόσημα στην ενίσχυση των δυνατοτήτων των τετράποδων ρομπότ για ποικίλα πραγματικά σενάρια.

Acknowledgements

I would like to begin by expressing my sincere gratitude to my dedicated supervisor, Prof. Panos Trahanias, whose unwavering guidance and support were invaluable throughout my time at the Computational Vision and Robotics Laboratory (CVRL, part of ICS-FORTH) and the University of Crete. Professor Trahanias's consistent encouragement and boundless enthusiasm served as a constant source of motivation, which was pivotal during the demanding research of the last two years that leaded to this MSc thesis. Professor Trahanias not only inspired me to pursue the MSc program but also consistently challenged me to acquire practical experience and develop the confidence necessary to excel in my early career journey. Professor Trahanias's mentorship has been an indispensable component of my academic progress, and I am truly indebted for his substantial role in my scholarly achievements.

In turn, I would like to heartfully acknowledge the contribution of Ass. Prof. Dimitris Papageorgiou to my academic journey. Prof. Papageorgiou's unwavering support and expert guidance have been instrumental in the development of my thesis. His discerning feedback and meticulous reviews enabled me to rigorously formulate my ideas. I am genuinely appreciative of the dedication and time he devoted to my project which had a direct impact on the quality of my work.

The role of Prof. Antonis Argyros in my graduate studies journey deserves special mention and appreciation. His apt comments and insights have greatly contributed in improving parts of this work. In addition, Prof. Argyros's teaching has been a source of inspiration and has impacted my academic temperament.

I would also like to express my gratitude to the University of Crete and especially the Computer Science Department (CSD). Through the outstanding Professors, classes and the enriching academic environment, I was able to both deepen and strengthen my knowledge during this master thesis.

It would have been a great omission if the Institute of Computer Science (ICS), Foundation for Research and Technology - Hellas (FORTH) was not acknowledged here. ICS-FORTH offered a vibrant research environment and access to cutting-edge robotics equipment, which greatly facilitated most of my research activities, such as development, evaluation, and testing. Furthermore, I gratefully acknowledge the financial support provided by ICS-FORTH all these years.

Moreover, I am truly thankful to the lab team of CVRL, for their unwavering dedication and support in fostering a friendly and inclusive environment. In particular, I want to express a special gratitude to Dr. Stelios Piperakis for his continuous and extraordinary support. His mentorship has been invaluable, and I am deeply appreciative of the impact he has had on my professional development. Also, I wholeheartedly express my gratitude to my colleague Michael Maravgakis for the numerous hours spent debugging code together, the extensive time dedicated to creative brainstorming and idea generation, as well as the countless moments of inspiration and idea development.

Lastly, the biggest "Thanks" to my family and friends, who have stood by me through thick and thin, enabling me to share these experiences with them!

to my parents,

Contents

List of Tables

List of Figures

Acronyms

BPMC Body Posture and Movement Controller. 1, 15, 45, 65

CLIK Closed-Loop Inverse Kinematics. 26, 35, 36

CNN Convolutional Neural Network. 12

CoM Center of Mass. 6, 7, 12, 13, 15, 19, 20, 21, 26, 33, 36, 39, 54, 57, 62, 66

FL Front-Left. 38, 39, 40

FR Front-Right. 38, 39, 59

IMU Inertial Measurement Unit. 23

KDE Kernel Density Estimation. 23

MPC Model Predictive Control. 12, 13, 67

PID Proportional Integral Derivative. 27

RL Rear-Left. 38, 39

RR Rear-Right. 38, 39, 41

ZMP Zero Moment Point. 6

Chapter 1

Introduction

In this chapter, we will delve into the realm of mobile robots, with a particular focus on legged robots, and more specifically, quadrupedal robots. These robots hold significant importance in various applications, as elaborated in this chapter. Our exploration will include an introductory overview of mobile robots, a comprehensive definition of legged robots in a broader context, and a detailed analysis of the importance of agile maneuvers and locomotion in challenging terrains for quadrupedal robots, which serves as the primary motivation for this work.

Subsequently, we will present the contributions of this thesis, which involve open-source software developed during this master's thesis, references to related publications, and an outline of the remaining content in this document.

1.1 Ground-based mobile robots

Within the field of ground-based mobile robotics, a common categorization places these robots into three key groups: wheeled, tracked and legged robots. Legged robots, notably, stand out due to their intricate design and sophisticated control systems, yet they excel in holonomic motion[1], maneuverability and versatile applications.

Unlike their counterparts as stated above, legged robots showcase the ability to adeptly navigate through complex, uneven terrains, surmount obstacles and ascend stairs efficiently while minimizing their impact on the ground. Among modern legged robots, which include bipeds, e.g (Fig. 1.1b) quadrupeds (Fig. 1.1a), hexapods and octopods, quadrupedal robots emerge as particularly noteworthy.

The advantages of legged locomotion hinge on various factors, including postures, the number of legs and leg functionality, as reviews on quadrupeds explain [1, 2, 3]. While wheeled and tracked robots are suitable for (almost) flat terrain, they

[1]The ability of a mobile system, to move freely and instantaneously in any direction within its workspace.

[2]`https://bostondynamics.com/products/spot/`

[3]`https://agilityrobotics.com/robots`

(a) Quadrupedal robot
Boston Dynamics[2]

(b) Bipedal robot
Agility Robotics[3]

Figure 1.1: Advanced industrial quadrupedal and bipedal robots.

often struggle in cluttered, complex, or hazardous environments. In contrast, legged robots possess the potential to navigate across diverse terrains, much like humans and animals. Animals utilize their legs for fast and reliable movement in various terrains, exhibiting exceptional locomotion and agility. They can adapt to environmental conditions with high speed and efficiency. From both stability and efficiency perspectives, the number of legs is by far significant.

Among legged robots, quadruped robots are particularly favored for their mobility and stable locomotion. Deploying four legs is more manageable in terms of control, design, and maintenance when compared to two or six legs. Researchers have been inspired by biological locomotion, particularly running gaits, which allow quadruped robots to handle significant payloads and maintain balance. Achieving real-time speed and natural movement, akin to animals like cows, dogs and cheetahs, necessitates the development of control systems and dynamic gait generation for quadruped robots.

1.1.1 Legged robots definition

Legged robots leverage their limbs for locomotion, as authors in [4] present, offering the unique benefit of an active suspension system [5]. The latter employs sensors and control algorithms to continuously adjust the leg movements and stiffness in real-time, enhancing stability and adaptability. This design allows for the robot's

primary body to be detached from the terrain's profile, providing exceptional adaptability to different landscapes. During each step, a leg is momentarily lifted from the ground, enabling the robot to navigate through rough or intricate terrain, effectively reaching otherwise inaccessible areas.

Typically, legs are composed of articulated rigid structures that establish contact with the environment primarily through their end-effectors. This contact is often one-sided, meaning that the robot can apply pushing forces but lacks the capability to exert pulling forces on contact surfaces. In certain scenarios, supplementary grip mechanisms like grasping, suction cups, magnets, adhesive materials or miniature spine arrays are implemented to enhance the robot's interaction with surfaces [1, 6].

In the pursuit of adapting wheeled vehicles to challenging terrains, a creative approach involves the integration of both wheels and legs [7], as Fig. 1.2 illustrates. These combinations can encompass various configurations of passive or active wheels and passive or active legs, capitalizing on the flexibility of articulated legs for traversing difficult terrain and the efficiency of wheels on smoother, level surfaces. Moreover, when confronted with steep slopes, legged robots have the option to employ rappelling as a technique to prevent potential tumbling incidents [8].

Figure 1.2: Force distribution among the legs of the quadruped robot.

1.1.2 Applications

Legged robots, particularly quadrupedal robots, have found diverse and valuable applications, with a strong emphasis on enhancing search and rescue operations

and inspection tasks. Versatile robotic systems excel in traversing challenging and hazardous environments, such as disaster-stricken areas, where traditional wheeled or tracked robots may struggle. Their four-legged design provides stability on uneven terrain, and their ability to climb over debris and navigate through cluttered spaces makes them ideal for locating and rescuing survivors in disaster scenarios. Additionally, quadrupedal robots are well-suited for industrial inspections, including inspections in confined spaces, hazardous environments, or infrastructure monitoring. Equipped with advanced sensors and autonomous capabilities, these robots are capable of collecting critical data and imagery, enhancing efficiency, safety, and precision in various inspection tasks. For instance, Cognite[4] and Aker BP[5] used Boston Dynamics' Spot robotic dog on the Skarv FPSO in the Norwegian Sea, e.g. Fig. 1.3. They employed Cognite's Cognite Data Fusion software as the data infrastructure for tasks such as autonomous inspection, data collection and report generation, sharing the collected data with Aker BP through a dashboard. As technology continues to advance, quadrupedal robots are poised to play an even more significant role in improving safety and efficiency in critical applications.

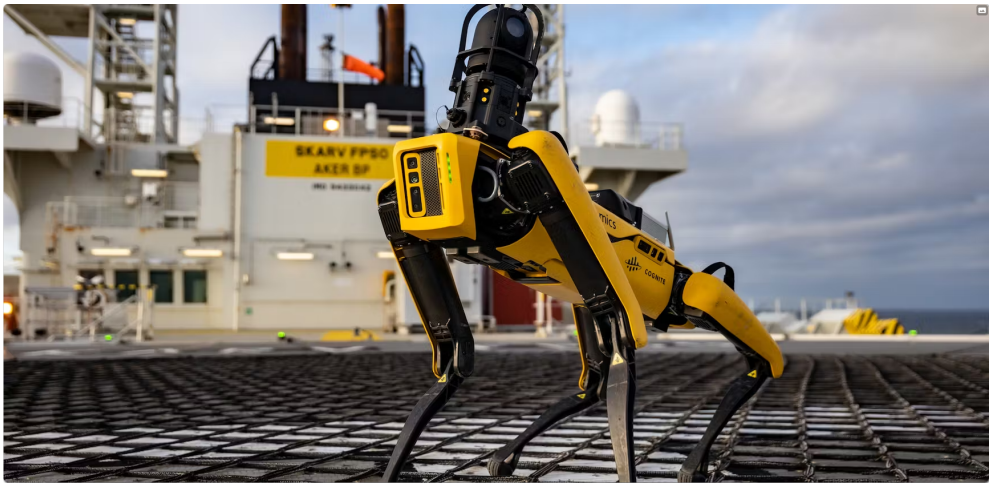

Figure 1.3: The Spot during inspection on the Skarv FPSO in the Norwegian Sea.

Legged locomotion has been studied and designed for the last couple of decades. Recent advances in both software and hardware have triggered the transition from experimental platforms used under laboratory conditions to (semi)autonomous machines deployed in real-world scenarios, e.g. on industrial sites for inspection [9] or in underground mines for exploration and mapping [10].

[4]A Norwegian software company that specializes in industrial data management and digitalization solutions

[5]A Norwegian oil exploration and production company

1.2 Trajectory tracking and locomotion in rough terrains

The main advantage of legged robots against other mobile robots, as previously mentioned, is their ability to discretize space [11], which enables them to traverse rough terrains, climb stairs and navigate in cluttered environments. Robots working in natural, urban and industrial settings need to be able to navigate challenging environments, safely, while keeping stability and controlability.

1.2.1 Motivation

Robotic locomotion in rough terrains presents a challenging research spectrum. During exploration, robots may inadvertently interact with structurally unstable and curved or spherical-shaped objects, such as pipes, which can lead to a loss of control. Additionally, navigating terrains featuring unpredictable friction properties, notably in low-friction settings like industrial areas with oil spills, poses another significant challenge.

In order to carry out tasks like navigating challenging terrains or attaining a particular body posture, it is crucial to carefully plan and implement a series of ground contacts, as highlighted in earlier research [12, 13]. Thus, achieving both nimble body postures and fluid movement requires the constant real-time assessment of each foot's contact status, that is, how securely it is positioned on the ground. At the same time, when considering the contact status, one must incorporate this information for recovery and adapt the overall body effort appropriately. This approach ensures both stability and the achievement of the desired task.

Detecting slippage right at its onset and swiftly regaining traction is a critical factor for maintaining body stability and can be the decisive factor in situations where falling is not a viable option. In fact, most locomotion and trajectory tracking controllers are built on the foundational assumption that the feet in contact with the ground are not experiencing slippage. Nonetheless, there are numerous instances during terrain exploration when slippage may arise, either due to slippery surfaces or as a result of the specific task's configuration.

In our research we introduce an adaptive controller for Body Posture and Movement, which overcomes the last mentioned restrictions. This controller factors in the contact status and guarantees stability by distributing effort based on weighted priorities, all while executing the desired task (trajectory tracking or locomotion) without sacrificing the spatial properties of the task.

1.3 Thesis contributions

The main contributions this work are:

- An adaptive trajectory tracking controller that equips the robot with a robust reactive behavior when it experiences slippage while ensuring its stability

and controllability without sacrificing the spatial properties of the desired trajectory.

- The proposed controller is theoretically proven to yield an asymptotically stable behavior.
- A novel target reaching controlling scheme that initiates agile movements and locomotion, through weighted pseudo-inverse matrix for stance foot selection.
- An adaptive target reaching controller that equips the robot with a robust reactive behavior when it experiences slippage while ensuring its stability and controllability during locomotion.
- We have performed extensive experimental evaluation of the proposed approach in various settings in both real and simulated scenarios with Unitree's GO1 quadruped robot (Fig. 1.4).

Figure 1.4: Unitree's Go1 quadruped robot dog.

Thesis Assumptions Significant contemporary research is devoted on improving the stability of robots while executing different gaits. A robot's stability can be characterized by its Center of Mass (CoM) location during static walking and Zero Moment Point (ZMP) during dynamic walking. A robot's posture is stable if its ZMP lies within a support polygon formed by the contact points of the legs in stance phase [14]. If the robot's body is close to the ground and its accelerations are small, we can approximate the ZMP location with the projection of the CoM

on the ground. Another assumption we make is the robot walks on a horizontal ground plane and its body attitude is kept horizontal. In that way, we can describe the projection of CoM as the current position of the CoM $(p_{c,x}, p_{c,y})$. In this work, unmodeled joint friction of motors, which has not been considered in the control scheme, serves as a disturbance to the system.

1.3.1 Open-source Software

In order to promote research and foster the incorporation of the proposed adaptive controller in body manoeuvres and locomotion schemes, this work has been released as an open-source module in ROS/C++ coined as *"Maestro"*. The name *"Maestro"* is inspired by the conductor of an orchestra, representing its central role in controlling and coordinating a legged robot's functions. The above-mentioned previous work on slip detection, namely the probabilistic contact estimator, can be found in "Probabilistic Contact Estimator":

- ROS/C++: Adaptive Body Posture and Movement Controller (Maestro)
  Author: Despina-Ekaterini Argiropoulos
  `https://github.com/despargy/maestro/` [15]
- ROS/Python: Probabilistic Contact Estimation (PCE)
  Author: Michael Maravgakis
  `https://github.com/MichaelMarav/ProbabilisticContactEstimation`
  [16]

1.3.2 Reference Publications

The first part of this thesis, the Adaptive Body Posture controller, has been accepted at the "Humanoids" conference scheduled for December $12 - 14$, 2023 [17].

> Despina-Ekaterini Argiropoulos, Dimitrios Papageorgiou, Michael Maravgakis, Drosakis Drosakis and Panos Trahanias, "Two-layer adaptive trajectory tracking controller for quadruped robots on slippery terrains", *2023 IEEE-RAS International Conference on Humanoid Robots*, Austin, Texas.

The research about probabilistic contact detection [16] was presented in ICRA 2023 conference, May 29 – June 2, 2023:

> Michael Maravgakis, Despina-Ekaterini Argiropoulos, Stylianos Piperakis, Panos Trahanias, "Probabilistic Contact State Estimation for Legged Robots using Inertial Information", *2023 International Conference on Robotics and Automation (ICRA)* , London, England.

In a relevant field of trajectory reconstruction and generalization, the following research work [18] has been presented in the 31^{st} IEEE International Conference on Robot and Human Interactive Communication (RO-MAN) 2022, Aug. 29 – Sep. 2, 2022:

Dimitrios Papageorgiou, Despina Ekaterini Argiropoulos, Zoe Doulgeri, "Dirichlet-based Dynamic Movement Primitives for encoding periodic motions with predefined accuracy", *2022 IEEE International Conference on Robot and Human Interactive Communication (RO-MAN)* , Naples, Italy.

A recent work submitted for presentation in ICRA 2024 about a novel method for path planning is the following:

Submitted for presentation:
Michael Maravgakis, Despina-Ekaterini Argiropoulos, Emmanouil Papadakis and Panos Trahanias, "Ray Casting and Diffusion Model for Path Planning of Mobile Robots in Static Environments", *2024 IEEE International Conference on Robotics and Automation (ICRA)*, YOKOHAMA, Japan.

1.4 Thesis outline

The outline of this thesis is structured into the following chapters, as explained below:

1. **Chapter 1 - Introduction**: This chapter serves as an introduction to legged robots, highlighting their significance and the challenges associated with traversing challenging terrains.

2. **Chapter 2 - Literature Review**: In this chapter, we provide a comprehensive review of recent works relevant to the field of this thesis.

3. **Chapter 3 - Methodology**: This constitutes the main chapter that features a detailed presentation of the proposed methodology.

4. **Chapter 4 - Experiments**: This chapter presents all the simulated and real experiments conducted to support the findings of this work.

5. **Chapter 5 - Conclusions**: In this final chapter, we discuss the outcomes and implications of this work and present ideas for future work.

6. **Chapter Appendix - Appendix**: This additional chapter contains proofs supporting the proposed method.

Chapter 2

Literature Review

Approaches for addressing trajectory tracking, agile manoeuvres and locomotion in challenging terrains, can be broadly categorized as either model-based or learning-based. In this chapter, we conduct an in-depth analysis of the strategies employed for task accomplishment in challenging terrains when firstly we present the problem description and our research focus. We take a multifaceted approach, starting with an exploration of how path planning methods tackle the challenge of traversing rough terrains. Following that, we delve into motion planning techniques. We also consider the role of proprioceptive feedback as a model-based approach in addressing this challenge through exploration of slip detection and recovery. Furthermore, we mention learning-based methods for tackling the complexities of terrain navigation. Additionally, we present recent advancements in trajectory tracking, which rely on the same underlying principle of successfully working in challenging terrains while accomplishing specific tasks, whether that entails safe walking or intricate maneuvers. Finally, we briefly present some conclusions regarding recent approaches to the problem of accomplishing tasks in challenging terrain.

2.1 Problem delineation and our research focus

One of the main advantages of legged robots is their capability to transverse unstructured environments, such as sewers or construction sites, which may involve a variety of challenging terrain types. This capability enables the utilization of legged robots in applications potentially dangerous for humans, such as search and rescue operations, inspection missions and maintenance in critical asset facilities. Further to their structural complexity, such difficult-to-transverse environments also impose dynamic challenges, with the most dominant being the variation of the friction coefficient of the terrain. Partially or globally slippery terrains are considered to be one of the most frequent problems faced by legged robots, which may arise in case of mud, wet floor, oil or ice [19]. Slippage of any leg with respect to the supporting surface could trigger unknown and unmodelled dynamics which would in turn worsen the trajectory tracking performance or even lead to robot's

instability; e.g. it could lead to singular configurations or to configurations in which the contact with the supporting surface is lost.

Slippage occurs when the magnitude of the tangential contact forces are outside the static friction cone, determined by the ratio of tangential to orthogonal force magnitudes (static friction coefficient). This coefficient, however, is difficult to model, varies in space and therefore, in most cases, is considered to be unknown a priori. To tackle the problem of identifying the slippage phenomenon, contemporary methods in literature propose the utilization of machine learning [20, 21, 22], classical estimators such as Extended/Unscented Kalman Filters [23, 24] and model-based estimators [25] which commonly utilize proprioceptive information to yield an estimate of the probability of stable contact, as proposed in our recent work [16].

Upon identification of slippage of one or multiple legs, a reactive behavior needs to be defined for ensuring the stability and controllability of the system. Common practices involve the utilization of estimators for slippage alongside with an online trajectory generation mechanism for slippage recovery.

Trajectory tracking is essential for dynamic locomotion on unstructured and slippery terrains. By tracking desired joint angles, foot positions and other kinematic variables, the robot can minimize energy consumption, improve speed and enhance maneuverability while maximizing stability and adaptability to different terrains.

2.2 Traversing rough terrains

Path Planning perspective Relying solely on path planning for terrain navigation does not entirely eliminate the risk of encountering challenging contact events. For instance, a recent study introduces an innovative approach that combines vision and proprioception to enhance legged robot navigation, particularly in quadrupedal robots[26]. While considering environmental conditions is crucial, it may not guarantee precise detection of forthcoming terrain conditions necessary for robot adaptation. Even with onboard range sensors such as laser range, time-of-flight, and stereo cameras, a robot can collect data on the terrain's geometry, yet it may not foresee potential contact between its end-effector and the ground. Moreover, these methods can be sensitive to environmental factors, including adequate lighting and the availability of visual or geometric features.

Motion planning Numerous motion planning strategies have been explored to address the challenge of rough terrain locomotion with quadrupedal robots, such as [27]. One approach centers on the identification of secure footholds and the execution of collision-free swing-leg motions, primarily by leveraging terrain mapping techniques[28]. In a recent development, terrain-aware motion optimization has emerged. This method jointly optimizes the robot's base pose and footholds, incorporating a height map and implementing a graduated optimization technique to circumvent local optima[29]. However, despite the promise shown by these

techniques in selecting appropriate footholds, they do not guarantee the prevention of potential slippage, which may lead to situations beyond the robot's control.

Proprioceptive feedback A model based work [30] presents a methodology for slip detection and estimation of the friction parameters, plus a recovery strategy which exploits the capabilities of a whole body controller, implemented for locomotion, which optimizes for the ground reaction forces. The estimation makes use only of proprioceptive sensors (no vision) as we use in this work. The recovery strategy is implemented at the force level and the idea behind the strategy is to correct the surface normal toward the estimated one resulting in ground reaction forces which were back inside the real friction cone.

One major limitations regarding the last mentioned method, is that as they say explicit, the estimated friction coefficient can only decrease during locomotion. Indeed, if the robot enters in a less slippery terrain after coming from a slippery one, it will keep the previous friction coefficient which will be too conservative. However, the same does not hold true for the state of locomotion, as robots often transition onto surfaces with varying friction levels.

Optimization techniques On the other hand, a multitude of studies have introduced optimization techniques to tackle the challenge of task accomplishment in diverse and challenging environments. In this context, many works have explored the use of (Hierarchical) Quadratic Programming methods for addressing dynamic functions with multiple constraints associated with a robot's stability and controllability.

Recent advancements in optimization methodologies, specifically those involving quadratic programming, have been well-documented. Notable contributions in this field can be found in references such as [31], [32], and [33].

In a work back in 2017[32], a trajectory optimization method for quadrupedal locomotion was introduced, capable of generating motion plans for different gaits, including walk, trot, and gait transitions. By integrating simple state-feedback laws and a hierarchical whole-body controller during motion execution, the robot could follow motion plans, even in the presence of disturbances or perturbations.

These methods are distinguished by their high complexity, relying on specific assumptions to reduce complexity and minimize computational requirements, thereby facilitating real-time application performance. Nonetheless, a noteworthy limitation of this approach is the need for pre-estimating the friction cones for upcoming contact point surfaces. Frequently, the friction coefficient remains unknown, posing challenges in accurate prediction before ground contact. Consequently, certain assumptions must be made regarding the friction cones, which may not be ideal for handling uncertain terrains with unknown surface types.

Learning models In the realm of learning-based approaches, novel methods have been devised to enhance the efficiency of quadrupedal robot locomotion across

challenging terrains, encompassing both indoor and outdoor environments such as icy surfaces, forests, and rocky landscapes. One notable contribution introduces a solution for integrating exteroceptive and proprioceptive perception in legged locomotion. The encoder is trained end-to-end, enabling the seamless fusion of diverse perception modalities without the need for heuristic methods. This results in a highly robust and speedy legged locomotion controller[34]. Additionally, a recent study proposes a learning-based technique to reconstruct local terrain information for mobile robots navigating urban settings. This approach leverages a continuous stream of depth measurements from onboard cameras, coupled with the robot's trajectory, to estimate the topography in the robot's immediate vicinity[35]. From motion planning approach, a study introduces a real-time foothold adaptation strategy that uses visual feedback and relies on onboard computers and sensors. This strategy continuously adjusts foot landing positions during leg swing phases and integrates a self-supervised foothold classifier based on a Convolutional Neural Network (CNN)[36].

In recent years, learning methods for locomotion have gained traction, yet they come with certain drawbacks. These include the need for substantial volumes of data to train models and a critical limitation - the absence of a foolproof formula to ensure desired outcomes; instead, we rely on learning metrics.

Model Predictive Control (MPC) MPC is a control strategy with the ability to predict future system behavior and make control decisions based on those predictions. It formulates an optimization problem to minimize a defined cost function while adhering to system constraints.

A comprehensive controller utilizing MPC was introduced in [7]. This work presents a whole-body MPC for hybrid locomotion, enabling online gait sequence adaptation. This approach optimizes the robot's torso and wheel motion as a single task, simultaneously optimizing joint velocity and ground reaction forces based on a kinodynamic model with moving ground contacts.

The framework presented in work [37] focuses on CoM control for position-controlled quadruped robots using a static walking gait. It utilizes MPC to manage the CoM's desired dynamics, with a key advantage being its ability to anticipate future states. This includes predictions of support polygon movements, allowing for adjustments to the CoM reference in anticipation of events such as leg liftoff.

Furthermore, there are works that combine MPC and learning methods, as seen in [38]. In their research, Reinforcement Learning is employed to establish a gait policy that adapts to diverse environmental conditions. MPC is then used to implement the chosen gait. To enhance locomotion robustness, a model adaptation policy is developed, dynamically optimizing input parameters for the MPC controller, ensuring adaptability and stability in various scenarios.

MPC stands as an advanced technique, supplying the controller with invaluable predictive insights for future control actions. Yet, the promise of amalgamating the dynamic model with real-time sensor data feedback and aligning the controller

accordingly holds the potential for substantial enhancements in adaptive control.

In contrast to MPC, we emphasize that real-time data processing enables us to adapt the robot's control effort promptly and ensure stability without the need to anticipate future time steps, as demonstrated by MPC methods.

2.2.1 Trajectory tracking

One study introduces a trajectory tracking control method aimed at enhancing the precision of tracking the trunk's CoM trajectory and foot-end trajectory in a fully electrically driven quadruped robot [39]. This method is composed of two main components: the trunk balance controller (TBC) and the swing leg controller (SLC). In the TBC, the method utilizes a dynamic model of the quadruped robot to determine the optimal foot-end force, which follows the trunk's CoM trajectory based on the MPC principle.

However, it's worth noting that this study does not consider the possibility of foot slippage. While the MPC method has the capability to anticipate future time-steps, it does not guarantee that the controller will have sufficient time to react and make adjustments in the event of unexpected contact, such as potential foot slippage, which may occur with one of the stance feet.

To the best of our knowledge, although some works tackle the problem of trajectory tracking for quadruped robots, such as [40] in joint space and [39] in task-space, the control problem is not explicitly addressed considering the operation on a partially or globally slippery terrain without sacrificing the task space trajectory.

2.2.1.1 Swinging leg trajectory

In this subsection, we will present pertinent references pertaining to the design of the swinging leg trajectory. This aspect holds significant significance as it constitutes a pivotal task in the locomotion that robots must undertake. Efficiency, encompassing considerations of time, energy utilization, and adaptability for foothold adjustments, is of paramount importance in this context.

In this paper[41], a swing leg trajectory optimization for a humanoid robot locomotion is presented. It is presented a straightforward and efficient approach to finding an optimal swing leg trajectory while adhering to physical joint limitations, employing a dynamic programming method. The trajectory's optimality is assessed based on a step traversal time criterion and accounts for the velocity and acceleration constraints of leg joints. These derived walking primitives, considering various walking parameters such as hip height, step size, and time, serve as a foundation for obtaining an optimal desired walking primitive with maximum robot velocity, all while adhering to predefined environmental constraints.

An other research, combing learning method, introduces an innovative high-level control system for dynamic quadruped robot locomotion [42]. It merges the rhythmic capabilities of Central Pattern Generators (CPGs) with foot trajectory

generation using Bézier curves. In that system, CPG output signals serve as driving parameters for a foot trajectory generator based on Bézier curves.

Bézier curves are commonly employed in numerous studies, including our current work, to define swinging leg trajectories. This choice is motivated by the advantageous properties of Bézier curves, particularly their derivative, which allows for the adjustment of foot speed during swing-leg retraction. This adaptability is beneficial in mitigating energy losses during running, as noted in the study by Haberland [43]. The utilization of Bézier curves in this context is instrumental in optimizing leg movement for improved energy efficiency during locomotion.

2.3 Conclusions

After conducting an extensive literature review on locomotion and agile maneuvers in challenging terrains, it becomes evident that there is a multitude of interesting works. The complexity of the problem and its multi-perspective nature make it challenging to encompass all potential failure cases in the real world.

Nonetheless, our proposed method, which integrates an adaptive body posture and movement controller, stands out as a novel approach. It not only minimizes the likelihood of slip detection but also introduces a new adaptive controller that takes into account the possibility of slippage with each step.

Chapter 3

Methodology

In this chapter, we present a comprehensive analysis of the proposed adaptive BPMC. The rest section begins with an overview of the problem statement, followed by introducing the conceptual solution for the BPMC, which we will subsequently detail in two distinct sections, as we will clarify later on. The primary objectives of the BPMC are twofold: firstly, to facilitate precise trajectory tracking in challenging slippery terrains, taking into account the slippage probability as discussed in our prior work[44], and secondly, to enable agile maneuvers and locomotion lying is the very same conceptual framework, as the first case, for slip detection.

The BPMC comprises two key components. The first is the "Body Posture Controller" for slippery terrains, which acts as a two-layer adaptive trajectory tracking controller for managing the CoM pose based on the given desired trajectory. The second component, known as the adaptive "Body Movement Controller", lays in the same conceptual framework to facilitate various movements and, simultaneously, initiate locomotion, even in simple or slippery terrains.

Both components of the adaptive BPMC controller exhibit the capacity to adapt and recover in response to slip detections, ensuring that safety is maintained and the successful completion of the desired task is not compromised.

3.1 Problem Formulation

Consider the quadruped robot depicted in Fig. 3.1, having $n \in \mathbb{N}$ joints in each leg and let $q_{i,j} \in \mathbb{R}, i = 1, ..., 4, j = 1, ..., n$ be the joint position variables of the i-th leg. Let $\mathbf{q} \triangleq [q_{1,1}\ q_{1,2}\ ...\ q_{4,n-1}\ q_{4,n}]^\intercal \in \mathbb{R}^{4n}$ be the vector of the total joint variables of the robot. Furthermore, let $\{C\}$ be the frame placed at the CoM of the robot (as depicted in Fig. 3.1) and ${}^c\mathbf{p}_i(q_{i,1}, ..., q_{i,n}) \in \mathbb{R}^3$ be the position of the tip of each leg with respect to $\{C\}$. The position and the orientation of $\{C\}$ with respect to the world frame $\{0\}$ is denoted by $\mathbf{p}_c \in \mathbb{R}^3$ and $\mathbf{R}_c \in SO(3)$ respectively. The world frame $\{0\}$ refers to a known inertial frame, or to the initial pose of the robot, namely $\{C\}$ at $t = 0$. Let $\mathbf{f}_c \in \mathbb{R}^3$ and $\boldsymbol{\tau}_c \in \mathbb{R}^3$ be the force and torque at the CoM respectively. The mapping between the ground reaction forces

$\mathbf{f}_i \in \mathbb{R}^3, i = 1, ..., 4$ applied to the tip of each leg and the corresponding generalized force $\mathbf{F}_c \triangleq [\mathbf{f}_c^\intercal \ \boldsymbol{\tau}_c^\intercal]^\intercal \in \mathbb{R}^6$ at the CoM, is the following:

$$\mathbf{F}_c = \mathbf{G}(\mathbf{q})\mathbf{F}_a, \tag{3.1}$$

where

$$\mathbf{G}(\mathbf{q}) \triangleq \begin{bmatrix} \mathbf{I}_3 & \mathbf{I}_3 & \mathbf{I}_3 & \mathbf{I}_3 \\ \mathbf{S}(\mathbf{p}_{c1}) & \mathbf{S}(\mathbf{p}_{c2}) & \mathbf{S}(\mathbf{p}_{c3}) & \mathbf{S}(\mathbf{p}_{c4}) \end{bmatrix} \tag{3.2}$$

and

$$\mathbf{F}_a \triangleq [\mathbf{f}_1^\intercal \ \mathbf{f}_2^\intercal \ \mathbf{f}_3^\intercal \ \mathbf{f}_4^\intercal]^\intercal \in \mathbb{R}^{12}, \tag{3.3}$$

with $\mathbf{p}_{ci}(q_{i,1}, ..., q_{i,n}) \triangleq \mathbf{R}_c {}^c\mathbf{p}_i(q_{i,1}, ..., q_{i,n}), i = 1, ..., 4$, $\mathbf{I}_3 \in \mathbb{R}^{3\times3}$ the identity matrix and $\mathbf{S}(.) : \mathbb{R}^3 \to \mathbb{R}^{3\times3}$ the skew symmetric mapping. Notice that $\mathbf{G}(\mathbf{q})$ belongs to $\mathbb{R}^{6\times12}$, and therefore the problem of solving for $\mathbf{F}_a$ given $\mathbf{F}_c$ from (3.1) is redundant. The mapping between the force applied to the tip of the i-th leg and the corresponding torques at the joints of the leg, is given by:

$$\boldsymbol{\tau}_i = (\mathbf{R}_c {}^c\mathbf{J}_i(q_{i,1}, ..., q_{i,n}))^\intercal \mathbf{f}_i, \tag{3.4}$$

where ${}^c\mathbf{J}_i(q_{i,1}, ..., q_{i,n}) \in \mathbb{R}^{3\times n}$ is the position part of the Jacobian of the leg with respect to the CoM and $\boldsymbol{\tau}_i \in \mathbb{R}^n$ the torques at the joints of the leg.

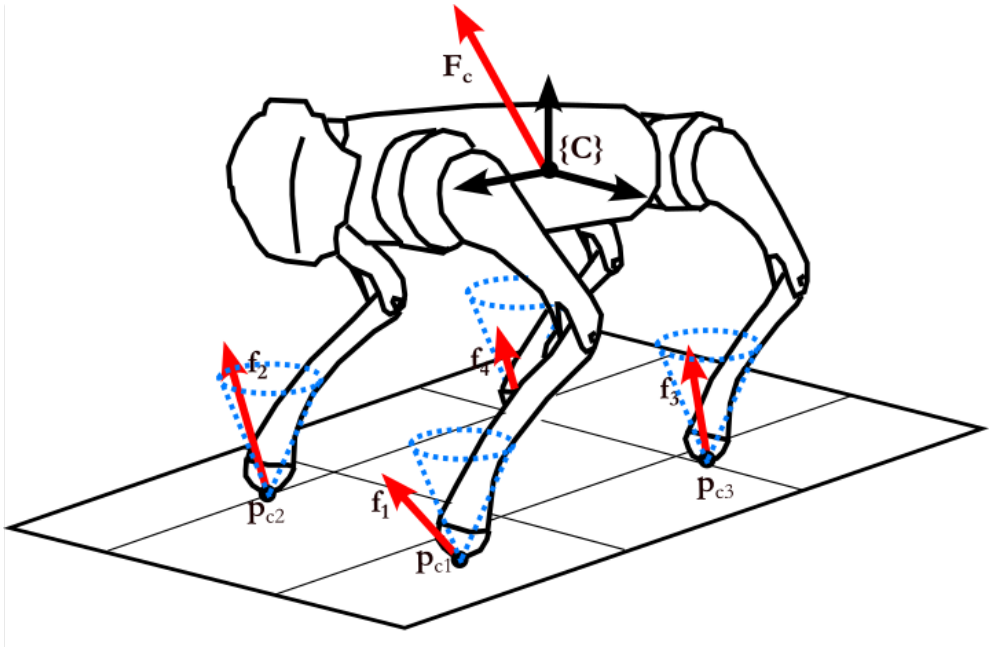

Figure 3.1: Force distribution among the legs of the quadruped robot.

Remark 1. *When less than four tips are in contact with the environment,* $\mathbf{G}(\mathbf{q})$ *has to be modified accordingly to involve only the legs that are in contact with the*

supporting surface. A representative example is in case of locomotion, in which one or more legs are in swing phase.

The dynamic model of the system, assuming that the inertia of the legs is negligible as compared to the inertia of the rest of the body, is given by:

$$\mathbf{H}_c\dot{\mathbf{V}}_c + \mathbf{C}_c\mathbf{V}_c + \mathbf{g}_c = \mathbf{F}_c, \tag{3.5}$$

where $\mathbf{V}_c \triangleq [\dot{\mathbf{p}}_c^\intercal \ \boldsymbol{\omega}_c^\intercal]^\intercal \in \mathbb{R}^6$ is the generalized velocity of $\{C\}$, $\boldsymbol{\omega}_c \in \mathbb{R}^3$ being its angular velocity, $\mathbf{H}_c \triangleq \text{diag}(m\mathbf{I}_3, \mathcal{I}_c) \in \mathbb{R}^{6\times6}$ is the positive definite inertia matrix of the robot, $\mathbf{g}_c \in \mathbb{R}^6$ the gravity vector and $\mathbf{C}_c \triangleq \text{diag}(\mathbf{0}_{3\times3}, \mathbf{S}(\mathcal{I}_c\boldsymbol{\omega}_c)) \in \mathbb{R}^{6\times6}$ the Coriolis-centrifugal matrix, with $\mathcal{I}_c \triangleq \mathbf{R}_c\mathcal{I}\mathbf{R}_c^\intercal \in \mathbb{R}^{3\times3}$ and $\mathcal{I} \in \mathbb{R}^{3\times3}$ the inertia tensor of the main body of the robot. In case the z-axis of the inertial frame is aligned to the gravity direction, $\mathbf{g}_c = [0\ 0\ m_r g\ 0\ 0\ 0]^\intercal$, with $m_r \in \mathbb{R}^+$ being the mass of the robot and $g \in \mathbb{R}^+$ the constant acceleration due to gravity. Notice that $\mathbf{a}^\intercal\left(\dot{\mathbf{H}}_c - 2\mathbf{C}_c\right)\mathbf{a} = 0, \forall\mathbf{a} \in \mathbb{R}^6$, which is the so called skew-symmetric property of the Lagrangian systems.

Consider a torque controlled robot which accepts joint torque commands $\boldsymbol{\tau}_i(t)$, where $\boldsymbol{\tau}_i(t) \in \mathbb{R}^n, i = 1, ..., 4$ are joint torques of the i-th leg. For solving the task-space trajectory tracking problem, one has to solve (3.1) with respect to $\mathbf{F}_a$, i.e. compute the inverse mapping, to calculate the forces that each leg should apply in order to render the commanded force in the task-space, $\mathbf{F}_c$, as follows:

$$\mathbf{F}_a = \mathbf{G}^\dagger(\mathbf{q})\mathbf{F}_c, \tag{3.6}$$

where $\mathbf{G}^\dagger \in \mathbb{R}^{12\times6}$ is the right pseudo-inverse of $\mathbf{G}$. In this point, there are multiple options regarding the pseudo-inverse. Some of them are the right Moore-Penrose pseudo-inverse, given by $\mathbf{G}^\dagger \triangleq \mathbf{G}^\intercal(\mathbf{G}\mathbf{G}^\intercal)^{-1}$, which will result in an equal distribution of control effort among the four legs (minimum norm solution), or the right weighted pseudo-inverse, given by:

$$\mathbf{G}^\dagger \triangleq \mathbf{W}^{-1}\mathbf{G}^\intercal(\mathbf{G}\mathbf{W}^{-1}\mathbf{G}^\intercal)^{-1}, \tag{3.7}$$

with $\mathbf{W} \in \mathbb{R}^{12\times12}$ being a positive definite weight matrix. The latter will result in distributing the control effort based on the selected weight matrix $\mathbf{W}$. More specifically, in this case, by selecting a positive definite diagonal matrix $\mathbf{W} \triangleq \text{diag}(w_{1,1}, w_{1,2}, w_{1,3}, ..., w_{4,3})$, the higher the $w_{i,m}$, the less the force appended to the m-th direction of the i-th leg's tip; for instance a high value of $w_{3,2}$ as compared to the other $w_{i,m}$-s, will result in appending less force along the y-direction ($m = 2$) of the third leg ($i = 3$). After computing the corresponding force in each leg, i.e. $\mathbf{f}_i$ which is included in $\mathbf{F}_a$, one can compute the commanded torques from (3.4).

Remark 2. *When the i-tip is in swinging phase or not in contact with the environment, one can assign infinitely large weights, denoted as $w_{i,1}, w_{i,2}, w_{i,3}$ to guide it towards the desired behavior. In such a case, there is no requirement to adjust $\mathbf{G}(\mathbf{q})$ to specifically include only the legs in contact with the supporting surface.*

3.1.1 The problem of slippage

From a control's perspective, dynamic contact events usually result in loss of controllability of the robotic system. In particular, slippage could lead a) to singular configurations, in which the rank of ${}^{c}\mathbf{J}_i(q_{i,1}, ..., q_{i,n})$ will be decreased, b) reaching the joint limits or c) losing contact in one or multiple legs without accounting for it, which is required for the validity of (3.6). As long as the force applied by each leg, i.e. $\mathbf{f}_i$, is within the friction cone, no slippage of the tip occurs, with respect to the supporting surface. More specifically, for a given terrain with constant static friction coefficient $\mu \in \mathbb{R}^+$, the static friction cone, which is the area in which there is not slippage, is expressed by:

$$\mathcal{C} \triangleq \{\mathbf{f}_i \in \mathbb{R}^3 : \mu|\mathbf{n}^\intercal \mathbf{f}_i| > ||(\mathbf{I}_3 - \mathbf{n}\mathbf{n}^\intercal)\mathbf{f}_i||\} \tag{3.8}$$

where $\mathbf{n} \in \mathbb{S}^2$, with $\mathbb{S}^2 \triangleq \{\mathbf{x} \in \mathbb{R}^3 : ||\mathbf{x}|| = 1\}$, is the normal to the supporting surface vector.

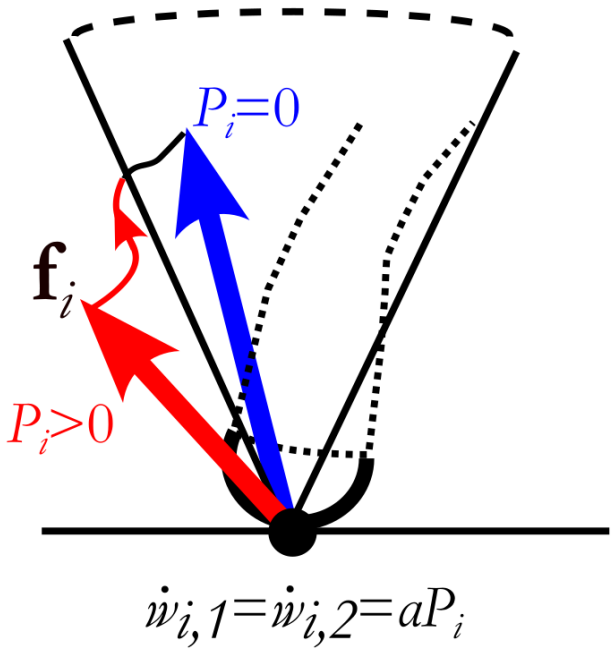

Figure 3.2: Convergence of the control effort of each leg towards the friction cone.

However, due to the fact that μ is not easy to measure or estimate and most of the times it is considered to be unknown, one cannot assess a priori, i.e. before commanding $\mathbf{f}_i$ to the leg, whether the leg's tip would slip or not.

3.1.2 The problem of agile movements

In the domain of control theory for agile movements and locomotion, ensuring stability revolves around the precise management of the robot's CoM in relation to the surface constructed by the tips of a quadruped robot's legs in contact with the ground. The geometric area outlined by the contact points of a quadruped robot's legs with the ground is called "support polygon". Ensuring that the projection of the CoM onto this support polygon remains within its boundaries is a pivotal factor in ensuring stability during the robot's agile movements and locomotion[45].

Mathematically, the support polygon can be described as a convex[1] polyhedron defined by the contact points between the robot's supported feet and the ground. Let S be the support polygon, and $\mathbf{p}_{c,i} \in \mathbb{R}^3$, for each i that refers to a supported feet with the ground. In Fig. 3.4, we may observe examples of the S area highlighted in blue, representing two different scenarios: (a) when all four feet are in contact with the ground, and (b) when the rear right leg is not in contact. At the same time, in each of the above cases, the center of support polygon changes, so the target we have selected for the CoM changes too, as we will later explain in more detail. Within Fig. 3.4, the variation in the position of the CoM is depicted as a green dot for each of these cases.

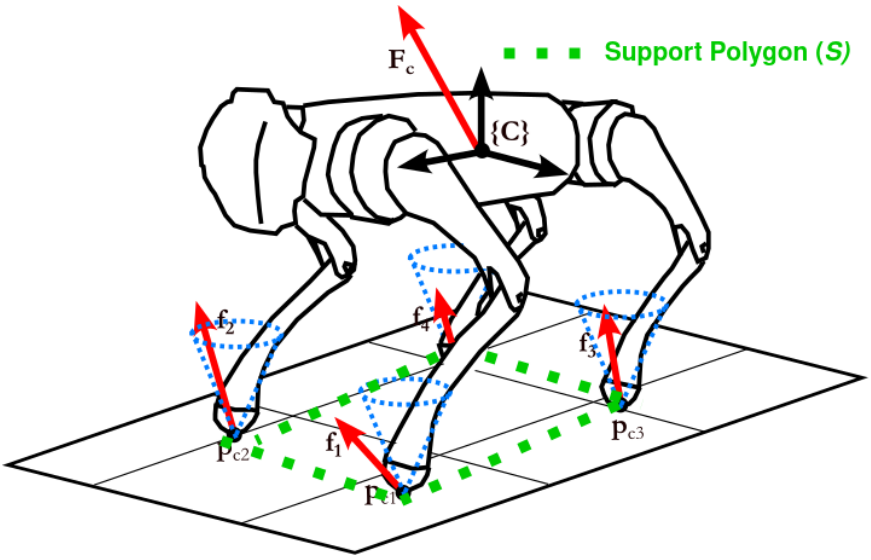

Figure 3.3: Support polygon definition with all supported legs on the ground.

The robot maintains stability during its motion as long as the projection of the position $\mathbf{p}_c$ of CoM onto the surface formed by the tip points remains within the boundaries of the support polygon. As the distance between the projection of the CoM and the center of the support polygon increases, the criticality of maintaining stability becomes more pronounced. A greater separation between these points

[1]Considering valid robot configurations limits

amplifies the challenges of balance and control, underscoring the need for precise and responsive control strategies to ensure the robot's stability during dynamic movements.

Ensuring that $\mathbf{p}_c$ remains within the support polygon during dynamic movements involves the design of control algorithms that regulate joint torques or control inputs in real-time. These algorithms utilize sensory feedback and predictive models to make rapid adjustments, ensuring that the robot's CoM stays well-positioned within the support polygon, thus preserving stability while enabling agile motions.

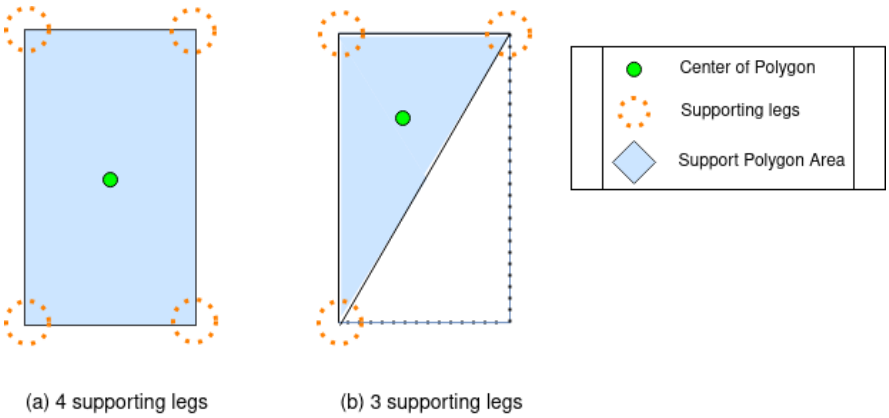

Figure 3.4: Center of Polygon example for cases: (a) 4, and (b) 3 supporting legs.

3.2 Concept Solution

Adaptive Body Posture Controller For the part of the adaptive Body Posture Controller, we propose a novel trajectory tracking control scheme featuring a two-layer online adaptation, based on the stable contact probability (counter proportional to the probability of slippage) derived from our previous work [44]. The first layer of adaptation introduces a weighted distribution of the control effort to the legs, by adjusting the 3D applied forces to the tip of each leg. The adaptive law utilizes the online-computed weights, based on the slippage probability of each leg. The rationale behind the first layer of adaptation law is to induce smaller tangential forces to the robot's end-effectors with large slippage probability in order to attract the force towards the fiction cone and prevent further slippage.

Furthermore, when the aforementioned force distribution cannot guarantee the elimination of slippage, we introduce the dynamic time-scaling of the trajectory in order to slow down the motion, namely, the second adaptation layer, which will consequently yield a reduced control effort magnitude in general. The complete adaptive control scheme is shown in Fig. 3.5.

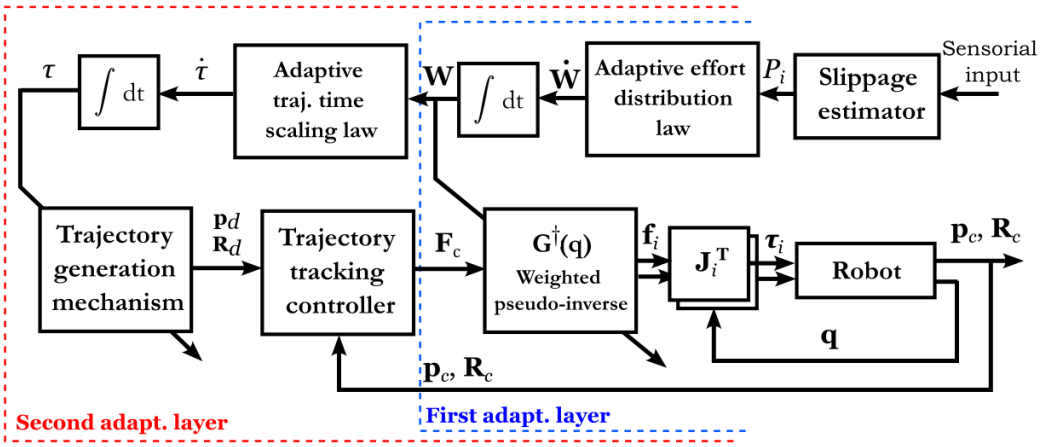

Figure 3.5: Block diagram of the Body Posture proposed adaptive scheme.

Body Movement Controller This section presents an innovative approach to agile movements and locomotion. We introduce an adaptive controller that leverages an unified concept for force distribution among the legs of a quadruped robot.

The Body Movement controller, serving as an adaptive reaching controller, plays a pivotal role in initiating locomotion tasks and executing agile maneuvers, particularly in challenging terrains marked by slipperiness and dynamic obstacles. The core of the Body Movement controller lies in its initial layer, in which the control effort is distributed among all stance legs, meaning all legs except the swinging leg. The latter is accomplished by assigning an exceptionally high weight to a specific leg, designated as the swinging leg. In that way, the swinging leg task is attained while, at the same time, the robot keeps its stability and controllability during locomotion.

Throughout this process, the controller consistently ensures stability by directing the CoM towards the center of the support polygon. The determination of the polygon's center takes into account only the legs that are in contact with the ground (stance legs) and the swinging leg is temporarily excluded from force distribution.

On top of that, the Body Movement controller offers an additional layer that can be activated at the user's discretion, taking into account the probability of detecting slip events. This extra layer draws inspiration from the approach used in the first layer of the Body Posture controller. It dynamically adjusts the effort distribution among all legs based on the slip probability of each foot. This multifaceted approach not only introduces innovative concepts for agile movements but also ensures the stability of the robot's dynamic maneuvers. It represents a crucial step in advancing the adaptability and robustness of the overall system. The complete adaptive control scheme for the Body Movement controller is shown in Fig. 3.6.

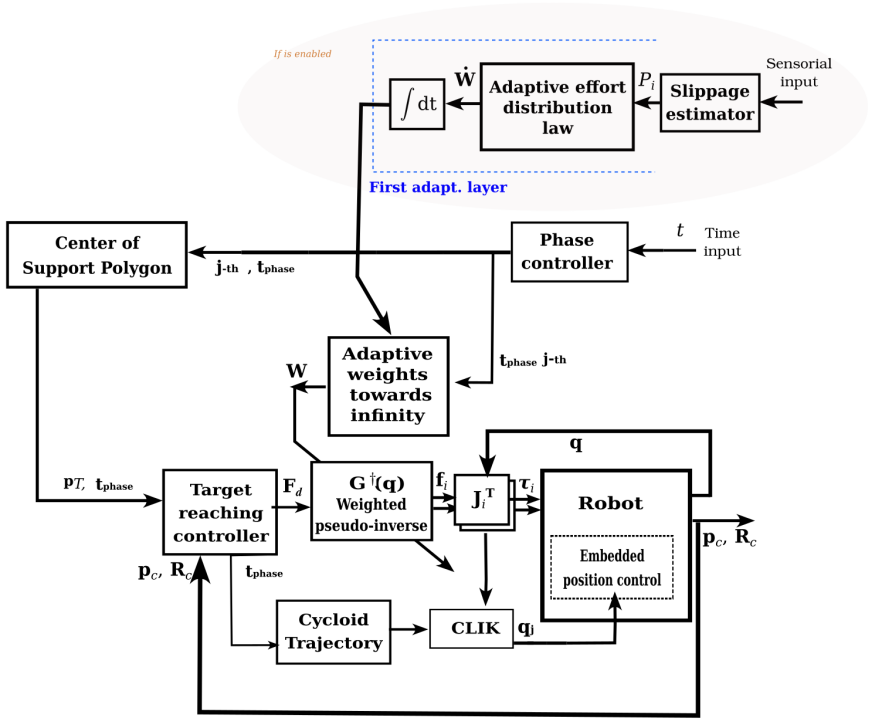

Figure 3.6: Block diagram of the Body Movement proposed adaptive scheme.

3.3 Adaptive Body Posture Controller

A novel trajectory tracking control scheme is proposed for quadruped robots, incorporating two prioritized layers of adaptation for minimizing possible slippage of one or multiple legs. The first layer of adaptation distributes the control effort among the legs without affecting the task performance, exploiting the redundancy of the quadruped robot. The second layer, which is activated only if the problem cannot be solved by the first layer, performs time-scaling of the trajectory which affects only the temporal properties of the task, without distorting the path followed by the robot. In other words, when the control effort distribution is not enough for tackling the problem of minimizing the slippage, the temporal scaling of the trajectory, meaning to slow down the motion, will lead to an overall reduction of the control effort that has to be applied by the robot's legs. Moreover, the proposed control framework builds upon our previous work[44] on contact state estimation and does not depend on friction cone estimates, as it would possibly require exploratory procedures which is one of the main advantages from methods

involving hierarchical quadratic programming and/or optimization with stack-of-tasks in general.

3.3.1 Proposed Scheme

Given a reference trajectory $\mathbf{p}_d(t) \in \mathbb{R}^3$ and $\mathbf{R}_d(t) \in SO(3)$ for frame $\{C\}$ in position and orientation respectively, we consider the trajectory tracking problem, i.e. the problem of minimizing the Euclidean norms of the following errors in time:

$$\mathbf{e}_p \triangleq \mathbf{p}_c(t) - \mathbf{p}_d(t), \quad \mathbf{e}_o \triangleq \log\left(\mathbf{R}_c(t)\mathbf{R}_d^\intercal(t)\right), \tag{3.9}$$

where $\log(\mathbf{R}) \triangleq \mathbf{k}\theta \in \mathbb{R}^3$ the logarithmic mapping, with $\theta \in [0, \pi]$ being the angle and $\mathbf{k} \in \mathbb{S}^2$ being the axis of rotation of a given $\mathbf{R}$. The trajectory $\mathbf{p}_d(t)$, $\mathbf{R}_d(t)$ could represent the motion of the main robot's body during its locomotion, or even dexterous motions for avoiding collisions in unstructured environments, e.g. the case of passing through a narrow opening.

Considering the system dynamics given in (3.5), the control objective can be achieved by applying the following state-feedback control law with gravity compensation, representing the commanded generalized force that should be applied to the CoM:

$$\begin{aligned}\mathbf{F}_c \triangleq & \mathbf{H}_c \begin{bmatrix} \ddot{\mathbf{p}}_d \\ \frac{d}{dt}\left(\mathbf{R}_c\mathbf{R}_d^\intercal\boldsymbol{\omega}_d\right) \end{bmatrix} + \mathbf{C}_c \begin{bmatrix} \dot{\mathbf{p}}_d \\ \mathbf{R}_c\mathbf{R}_d^\intercal\boldsymbol{\omega}_d \end{bmatrix} \\ & - \begin{bmatrix} k_p\mathbf{e}_p \\ k_o\mathbf{e}_o \end{bmatrix} - \mathbf{K}_v\mathbf{e}_v + \mathbf{g}_c,\end{aligned} \tag{3.10}$$

where

$$\mathbf{e}_v \triangleq \mathbf{V}_c - \begin{bmatrix} \dot{\mathbf{p}}_d \\ \mathbf{R}_c\mathbf{R}_d^\intercal\boldsymbol{\omega}_d \end{bmatrix}, \tag{3.11}$$

$k_p, k_o \in \mathbb{R}^+$, $\mathbf{K}_v \in \mathbb{R}^{6\times6}$ are constant positive control gains and $\boldsymbol{\omega}_d \in \mathbb{R}^3$ is the reference angular velocity which can be calculated by $\mathbf{S}(\boldsymbol{\omega}_d) = \dot{\mathbf{R}}_d\mathbf{R}_d^\intercal$. The proof of global asymptotic stability of the origin of the state-space, corresponding to zero error in position and velocity, under the application of the control law (3.10), is proven in Appendix 5.1.

3.3.2 Slippage detection

For the slippage detection mechanism, stable contact is considered to be the state in which the robot's foot is in touch with the ground whilst there is no relative motion between them. To estimate the stable contact probability, a 6D Inertial Measurement Unit (IMU) sensor is mounted on each foot of the robot. By exploiting the uncertainty of the inertial measurements, we employ Kernel Density Estimation (KDE) to approximate the Probability Density Function for each axis of the IMU and consequently the per axis stable probability over a small interval, as dictated in [44]. The method, practically estimates the probability that the

inertial measurements are close to zero and finally, since they are independent, the total stable probability is acquired via multiplication. Finally, in order to detect when the foot touches the ground, one can utilize force measurements, haptic or dedicated contact sensors. To this end, in this work we exploited the vertical force measurement ($f_{i,z} > 0$).

3.3.2.1 First layer of adaptation: Adaptive effort distribution

Based on the above slippage detection mechanism, we propose the following adaptive law for the weights $w_{i,m}, m = 1, 2$ (the $x - y$ coefficients) of the tangential force directions of the i-th leg:

$$\begin{aligned} \dot{w}_{i,1} = \dot{w}_{i,2} &\triangleq \alpha P_i, \\ w_{i,1}(0) = w_{i,2}(0) &\triangleq w_0 \end{aligned} \tag{3.12}$$

where $\alpha \in \mathbb{R}^+$ is a tunable constant adaptation gain, $w_0 \in \mathbb{R}^+$ the initial value of the weights in $x - y$ direction and $P_i \in [0, 1]$ the probability of slippage of the i-th leg. Notice that the normalization of $w_{i,m}, i = 1, ..., 4, m = 1, 2, 3$ is not required, as (3.6), (3.7) do not assume constraints for the values of $\mathbf{W}$.

Remark 3. *As the update law (3.12) involves only positive derivatives of the weights, the weights require re-initialization between consecutive footholds, as the surface properties of the new contact point are considered unknown.*

Remark 4. *Notice that (3.12) assumes the orthogonality between the supporting surface and the gravity direction, for the sake of simplicity of presentation. However, the generalization to inclined surfaces can be easily done by considering a non-diagonal* $\mathbf{W}$ *matrix.*

Remark 5. *Given (3.12), the weights will increase only as long as slippage is estimated, which means that the weights will eventually reach the value in which the control effort appended to the specific leg does not yield any slippage. The increase of these weights (i.e. the weights corresponding only to the tangential forces) will result in decreasing the magnitude of forces appended towards these directions. Therefore, the appended force* $\mathbf{f}_i$ *will converge to the friction cone* $\mathcal{C}$*, as graphically depicted in Fig. 3.2.*

3.3.2.2 Second layer of adaptation: Trajectory time-scaling

When all supporting legs are slipping, the first adaptation layer may be insufficient to restore the robot's stability. Hence, to handle this type of occasions, we propose the time-scaling of the trajectory which sacrifices the temporal accuracy of the task for guaranteeing stability and controllability, maintaining however accuracy with respect to the spatial properties of the path.

Let $\mathbf{p}_d(t_v), \mathbf{R}_d(t_v)$ be the time-parametric trajectory, with $t_v(t) \in \mathbb{R}^+$ being the scaled time parameter and $\beta \in [0, 1]$ the time-scaling coefficient. Hence, the

evolution of the scaled time parameter is characterized by $\dot{t}_v(t) = \beta(t)$. For instance, setting a constant $\beta = 1$ would result in $t_v = t$ and consequently would lead to the execution of the trajectory on a nominal speed, while setting $\beta < 1$ would slow down the motion. To tackle the problem of global slippage, we propose the utilization of the following time-scaling coefficient:

$$\beta(t) \triangleq \frac{w_0}{\min(w_{1,1}, w_{2,1}, w_{3,1}, w_{4,1})}. \tag{3.13}$$

The rationale behind (3.13) is to reduce the speed (reflected by β) when slippage has occurred in all four legs, an occasion which is signified by the increase of the weights of all four legs due to (3.12). For instance, if at least one of the legs does not face any slippage, then $\min(w_{1,1}(t), w_{2,1}(t), w_{3,1}(t), w_{4,1}(t))$ will be equal to w_0 and therefore β will be 1, which means that no time scaling would occur.

As the online time scaling is considered, the trajectory should be generated online from t_v, which is calculated by the integration of $\dot{t}_v = \beta(t)$ in real-time. Notice that, in such a case $\dot{\mathbf{p}}_d(t) = \beta(t)\frac{d\mathbf{p}_d(t_v)}{dt_v}, \dot{\mathbf{R}}_d(t) = \beta(t)\frac{d\mathbf{R}_d(t_v)}{dt_v}$. The complete algorithm of the proposed control scheme is given in Algorithm 1.

Remark 6. *Notice that if the trajectory is generated online by a dynamical system (e.g. a Dynamic Movement Primitives model [46]), the application of the aforementioned idea is straight forward, as in that case β would correspond to the time scaling parameter of the dynamical system.*

Algorithm 1 Implementation of the control loop - Body Posture

1: Select values for: $k_p, k_o, \mathbf{K}_v, w_0$
2: $\mathbf{W} := w_0\mathbf{I}_{12}, \beta := 1, t_v := 0$ ▷ Initialization
3: **while** control is enabled **do**
4: Get current state of the robot $\mathbf{p}_c, \mathbf{R}_c, \dot{\mathbf{p}}_c, \boldsymbol{\omega}_c$
5: Estimate $P_i, \forall i = 1, ..., 4$ ▷ Slip. prob. estimator
6: Compute $\dot{w}_{i,1}, \dot{w}_{i,2}, \forall i = 1, ..., 4$ from (3.12)
7: Integrate $\dot{w}_{i,1}, \dot{w}_{i,2}, \forall i = 1, ..., 4$ to update $\mathbf{W}$
8: Compute β from (3.13)
9: Integrate $\dot{t}_v = \beta$ to update t_v
10: Compute $\mathbf{p}_d(t_v), \dot{\mathbf{p}}_d(t_v), \ddot{\mathbf{p}}_d(t_v), \mathbf{R}_d(t_v), \boldsymbol{\omega}_d(t_v), \dot{\boldsymbol{\omega}}_d(t_v)$
11: Compute $\mathbf{F}_c$ from (3.10)
12: Compute $\mathbf{F}_a$ (includes the $\mathbf{f}_i$-s) from (3.6), (3.7)
13: Compute $\boldsymbol{\tau}_i, \forall i = 1, ..., 4$ from (3.4)
14: Command $\boldsymbol{\tau}_i, \forall i = 1, ..., 4$ to the joints
15: **end while**

Remark 7. *To additionally account for tasks that involve deliberate contact loss of the foot, such as swinging, during trajectory tracking, we propose the utilization*

of the following smooth fade-out function for the weights of the specific leg (the i-th leg) that is about to elevate:

$$w_{i,m}(t) = \begin{cases} w_{i,m}(0) + atanh\left(\frac{t}{t_f}\right), for\, t \leq t_f \\ \infty, \ otherwise \end{cases} \tag{3.14}$$

where $t_f \in \mathbb{R}^+$ is the predefined fading-out duration and $m = 1, 2, 3$; we consider $t = 0$ being the instance at the start of the event. Based on (3.14), after t_f, the i-th leg will not be taken into account for the solution of (3.1) and it will not be considered within the minimum function of (3.13), as its weights will reach infinity.

3.4 Body Movement Controller

In this section, we delve into an elaborate explanation of the Body Movement controller, which shares the same foundational concept as its predecessor. This controller assumes the dual role of overseeing agile motions and initiating locomotion, all while upholding stability by guiding the CoM towards the center of the support polygon.

The central idea here is a controller that seamlessly balances stability and the execution of specific tasks for individual legs, such as locomotion. To achieve this balance, we employ a dynamic weight adjustment strategy for the designated swinging/task-desired leg j, represented as $w_{j,1}, w_{j,2}, w_{j,3}$. By driving these weights towards a notably high value, the corresponding leg effectively exits the torque distribution solution (3.6).

In the context of this controller, we have defined a free gait, to determine the order of swinging each leg to initiate locomotion. During this phase, the leg in the swinging motion is controlled using a Closed-Loop Inverse Kinematics (CLIK) approach and follows a given desired swinging trajectory. Throughout this process, the controller consistently guarantees stability, enabling the swinging legs to execute the desired motions with precision and reliability, while the CoM is reached the center of the support polygon.

3.4.1 Proposed Scheme

Given a desired target $\mathbf{p}_t \in \mathbb{R}^3$ and $\mathbf{R}_t \in SO(3)$ for frame $\{C\}$ in position and orientation respectively, we consider the reaching target problem, i.e. the problem of minimizing the Euclidean norms of the following errors in time:

$$\mathbf{e}_p \triangleq \mathbf{p}_c(t) - \mathbf{p}_t, \quad \mathbf{e}_o \triangleq \log\left(\mathbf{R}_c(t)\mathbf{R}_t^\intercal\right), \tag{3.15}$$

where $\log(\mathbf{R}) \triangleq \mathbf{k}\theta \in \mathbb{R}^3$ the logarithmic mapping, with $\theta \in [0, \pi]$ being the angle and $\mathbf{k} \in \mathbb{S}^2$ being the axis of rotation of a given $\mathbf{R}$. The target $\mathbf{p}_t$, $\mathbf{R}_t$ could represent the center of support polygon of the main robot's body during its locomotion or agile movements.

Considering the system dynamics given in (3.5), the control objective can be achieved by applying the following state-feedback control law with gravity compensation and integral term, representing the commanded generalized force that should be applied to the CoM:

$$\mathbf{F}_c \triangleq -\begin{bmatrix} k_{i,p} \cdot \text{sat}\left(\int_0^t \mathbf{e}_p dt\right) \\ k_{i,o} \cdot \text{sat}\left(\int_0^t \mathbf{e}_o dt\right) \end{bmatrix} - \begin{bmatrix} k_p \mathbf{e}_p \\ k_o \mathbf{e}_o \end{bmatrix} - \mathbf{K}_v \mathbf{e}_v + \mathbf{g}_c, \tag{3.16}$$

where

$$\mathbf{e}_v \triangleq \mathbf{V}_c, \tag{3.17}$$

$k_p, k_o, k_{i,p}, k_{i,o} \in \mathbb{R}^+$, $\mathbf{K}_v \in \mathbb{R}^{6\times 6}$ are constant positive control gains and sat() a saturation function to bound the position into the support polygon bounds.

In contrast with the previous controller, in this scenario, there is no desired velocity and acceleration, as we have a reaching problem. Then, the initial two terms in equation 3.10 are no longer relevant. This implies that $\ddot{\mathbf{p}}_t = 0, \dot{\mathbf{p}}_t = 0, \boldsymbol{\omega}_t = 0$. Additionally, we've introduced a integration term, denoted as k_i. This parameter is set to unity for both position, denoted as $k_{i,p}$, and orientation, denoted as $k_{i,o}$, to aid in achieving the target objective.

Firstly, the integral gains $k_{i,p}$,$k_{i,o}$ in the Proportional Integral Derivative (PID) controller are exceptionally handy for dealing with persistent errors that linger even after changes in the system. It continually adds up these errors over time and helps make the necessary adjustments to steer the system toward its target, even when there are hiccups or uncertainties.

Additionally, the integration feature in the PID controller acts like a safety net to ensure that the control commands don't go beyond certain limits. This is vital in systems with physical boundaries or safety requirements. It ensures that the system's actions stay in a safe and stable range, avoiding situations where things go too far or get too unstable.

3.4.1.1 Adaptive weights towards an exceedingly high value

In the scenario where leg j is engaged in a specific task(e.g., swinging), whether in joint or task space, to maintain the robot's stability, the control effort of the posture controller should be directed to all legs except for j-th leg.

As pointed out in Remark 1, this would typically entail manual adjustments to $\mathbf{G}(\mathbf{q})$, where only the legs in contact with the ground are considered. However, as proposed in Remark 2, a more streamlined approach can be adopted. Instead of altering $\mathbf{G}(\mathbf{q})$, we simply adjust the weights associated with leg j to an exceedingly high value. In this situation, these weight adjustments tend toward a considerably high value, effectively minimizing the control effort distribution for leg j.

In greater detail, the goal for the adaptive weights associated with the selected leg is to gradually approach a considerably high value during a specified time window

when the robot is actively performing the designated task for that leg. During this period, the control effort is redirected to the other legs, as previously mentioned. To achieve this dynamic behavior, we utilize the super-Gaussian function, which enables the weights to rapidly rise to predetermined levels, w_{max}, within the defined time window before reverting to their initial values w_0.

Super-Gaussian

- **Performance Customization:** Super-Gaussian functions provide more flexibility in shaping their performance characteristics. Unlike the classic Gaussian function, which has a fixed and symmetrical shape, super-Gaussian functions can be adjusted to take on various shapes and behaviors. This adaptability allows us to fine-tune the function to better suit the requirements of the task for the selected leg.

- **Controlled Asymptotic Behavior:** Super-Gaussian functions are particularly useful when you need precise control over the rate at which the function approaches its peak value, as we currently need for the adaptive weights. By modifying the function's higher-order moments, one can control the shape of the curve, influencing how quickly it reaches a chosen value and how it behaves in the tails. This control is valuable for modeling various distributions and characteristics. The final scenario occurs when we need to execute a task rapidly and with precise adaptability using the selected leg. For instance, in a scenario where a leg needs to start swinging, the rate at which control is transferred may determine how quickly the leg transitions from its current state to the swinging motion, or how smoothly it assumes control of the swinging action. This rate can be adjusted based on the specific requirements of the task and the robot's performance goals.

- **Time Window for Performance:** One notable advantage associated with the super-Gaussian function is its capability to attain specific values within specified time intervals. This sets it apart from the Gaussian function, which maintains a consistent standard deviation regardless of the desired value. In contrast, super-Gaussian functions can be tailored to swiftly reach a targeted value within a defined time frame. This feature holds significant importance in applications where time-sensitive responses are critical, such as tasks involving leg swinging. The performance within this time window plays a pivotal role in determining the duration of the swinging leg's motion.

The duration or lifespan of a super-Gaussian function is determined by its specific mathematical formulation and parameters. In this implementation, we use the super-Gaussian function, of the following form (3.18), as it is presented and well explained in [47]:

$$G(x,y) = A \cdot \left(b^{-\left(\frac{d(x,y)^2}{r^2}\right)^P} \right) \tag{3.18}$$

where A, b, P, $r = \frac{A}{b}$ are parameters $\in \mathbb{R}^+$ and $d(x,y)$ is a distance function. Furthermore, it can be observed that $G(d = r) = \frac{A}{b}$. The properties of the super-Gaussian function are illustrated in Fig. 3.7.

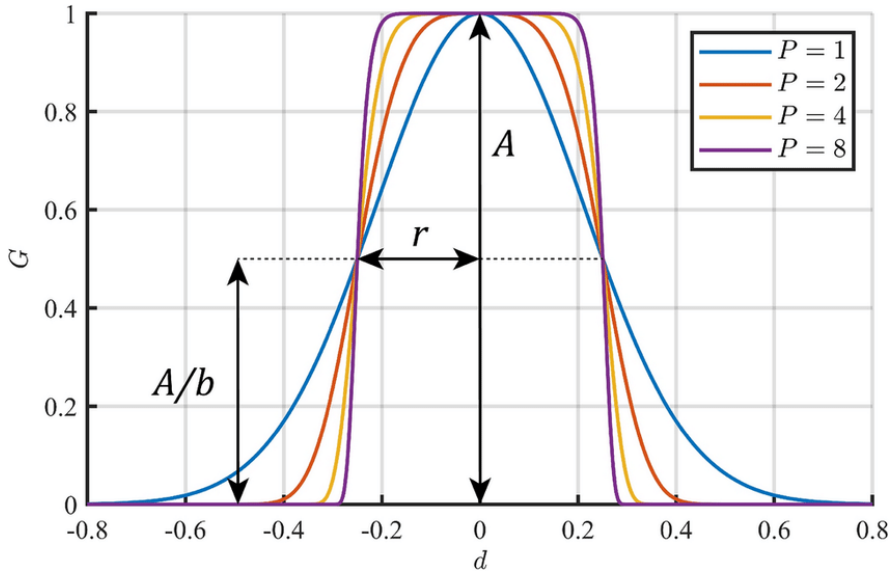

Figure 3.7: Profile of the super-Gaussian beam for various values of parameter P.

The super-Gaussian function presents a plateau-shaped top, featuring a smooth Gaussian decay along the directions of increasing distance represented by the function $d(x,y)$. Within this context, specific parameters assume distinct roles:

1. The parameter P plays a pivotal role in governing the sharpness of the plateau. It essentially controls how swiftly the function transitions from zero to its peak and subsequently returns to zero.

2. In parallel, the coefficient A serves as a determinant of the plateau's height, signifying the function's maximum value at its peak.

3. Furthermore, the radius parameter r carries notable significance, as it defines the length from the plateau's center to a point within the fall-off region. This length is expressed as a ratio of the height A divided by the base parameter b.

In essence, these parameters collectively shape the distinct features of the super-Gaussian function, including the sharpness of its plateau, its peak height, and the dimensions of its fall-off region concerning its center.

In this particular implementation aimed at initiating locomotion, we have selected specific parameter values: $A = 1$, $b = 10$, and $n = 13$. The resulting performance is illustrated in Fig. 3.8. Let t_{phase} be the current time for the phase of swinging leg, t_0 signifies the time at which the super-Gaussian function starts activating and reaches a small value of 0.1, and t_{half} represents the midpoint of the high-value time window within the function. Thus, the super-Gaussian function that was selected for the Movement controller is given by:

$$superG(t_{phase}) = A \cdot \left(b^{-\left(\frac{(t_{phase}-t_{half})^2}{(t_{half}-t_0)^2}\right)^{n\cdot(t_{half}-t_0)}} \right) \tag{3.19}$$

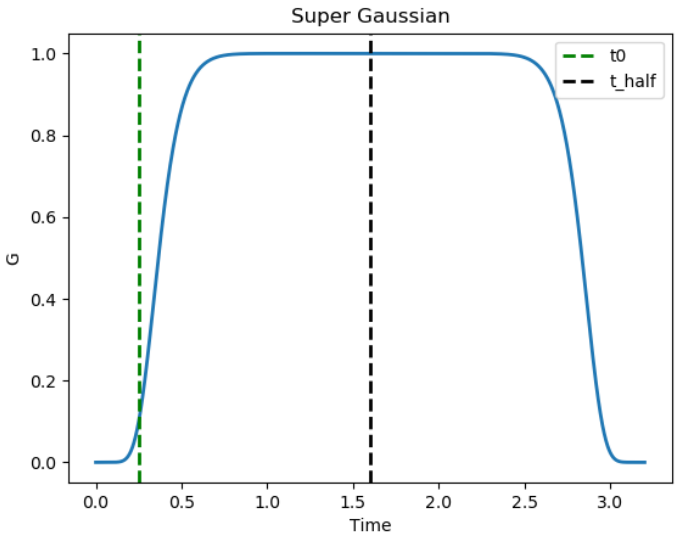

Figure 3.8: Desired Super-Gaussian performance.

The desired performance for the adaptive weights can be described as follows. When the j-th leg is selected as the swinging or task-desired leg, its initial weight is denoted as w_0. As indicated in Remark 2, this weight needs to be adjusted, transitioning from the initial value w_0 to a significantly higher value w_{max} and then returning to w_0 once the desired task is completed. To implement this weight adaptation, we utilize the following equation, incorporating the super-Gaussian function described in Equation (3.19):

$$w_{j,m} = w_0 + w_{max} \cdot superG(t_{phase}) \tag{3.20}$$

where $m = 1, 2, 3$ for each axis x, y, z. The desire performance of weights over a high value during one cycle of locomotion is displayed in Fig. 3.9:

,where $w_0 = 35, w_{max} = 3500$ for x-axis. It's important to note that this identical performance applies to both the y-axis and z-axis as well.

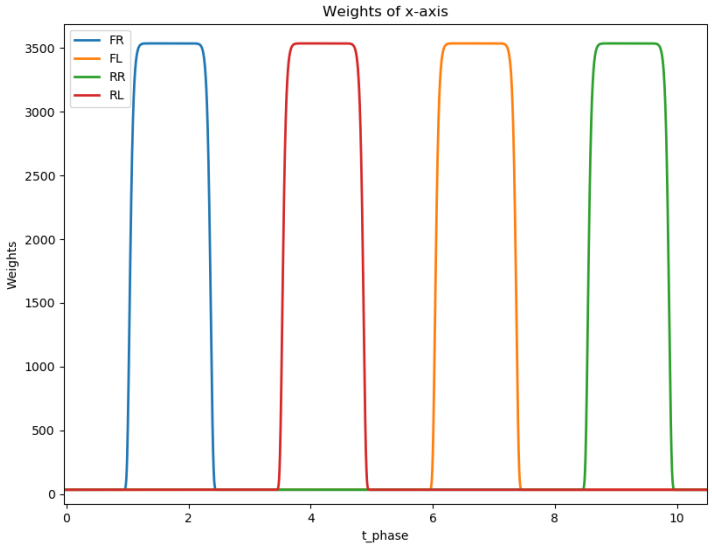

Figure 3.9: Adaptive weights during one cycle of locomotion.

3.4.1.2 Swinging phase

The assessment of our approach's effectiveness in agile movements and locomotion primarily revolves around the task of leg swinging. As detailed in the forthcoming "free gait" section (Section 3.4.1.3), we have devised a comprehensive gait planning strategy to initiate locomotion. This locomotion process is partitioned into four distinct phases, each corresponding to a specific leg. Within this chapter, our focus revolves around the comprehensive performance analysis of swinging leg j. This analysis serves as a foundational step that can subsequently be extended to encompass the evaluation of each of the robot's legs.

In the swinging phase, we've chosen to utilize (a) a cycloid trajectory and (b) a 3-rd order Bezier curve as swinging trajectory, to govern the movement of each leg's end-effector.

Each trajectory is defined by a specific time duration. We introduce cycloid trajectory since its simplicity, and when, the choice of a Bezier trajectory for swinging legs is coming as a strategic decision aimed at optimizing motion quality, energy efficiency, timing coordination, mechanical durability, and stability—all essential factors in achieving effective agile movements and locomotion for quadruped robots [43], as it is explained in details in the following paragraph of "Bezier curve".

It's important to emphasize that our primary interest lies in the tip's trajectory along the x and z axes. We specifically focus on the two-dimensional desired swinging trajectory that the tip follows within this plane.

Cycloid trajectory This trajectory, which unfolds in the x-z plane, is characterized by Equations 3.21:

$$\begin{aligned} x(t_{phase}) =& r1 \cdot \Big(2 \cdot \pi \cdot \text{freq\_swing} \cdot (t_{phase} - t_{0,swing}) \\ & - \sin\big(2 \cdot \pi \cdot \text{freq\_swing} \cdot (t_{phase} - t_{0,swing})\big) \Big) \\ z(t_{phase}) =& r2 \cdot \Big(1 - \cos\big(2 \cdot \pi \cdot \text{freq\_swing} \cdot (t_{phase} - t_{0,swing})\big) \Big) \end{aligned} \tag{3.21}$$

where $r1, r2 \in \mathbb{R}$ are distance parameters, freq_swing $\in \mathbb{R}$ is the frequency of the cycloid trajectory. Consider $t_{phase} \in \mathbb{R}$ as the time counter of a single swinging phase for leg j, and let $t_{swing\_slot} \in \mathbb{R}$ represent the target duration for each swinging phase. Consequently, $t_{phase} \in [0, t_{swing\_slot}]$ since it resets to zero at the commencement of each new phase, signifying the cyclic nature of the swinging leg transitions. One can define $t_{0,swing}$ as the specific moment when the cycloid trajectory is intended to become active.

Fig. 3.10 illustrates the time-dependent cycloid trajectory over x and z axis, as an example, where $t_{swing\_slot} = 2.9, t_{0,swing} = 0.6, \text{freq\_swing} = 0.5, r1 = 0.01, r2 = 0.02$.

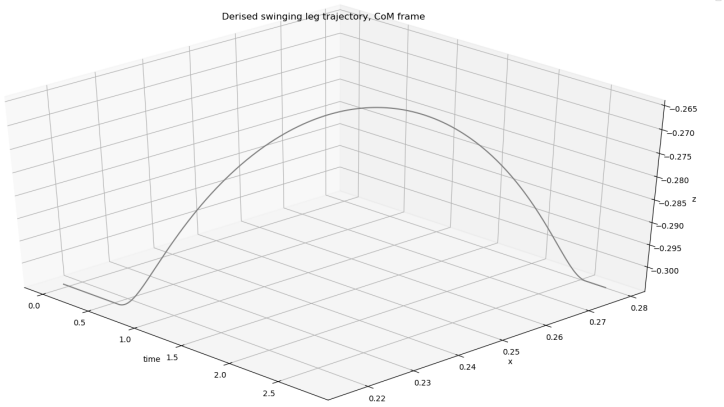

Figure 3.10: Desired swinging leg trajectory, refer. CoM.

Through differentiation, one can determine the desired velocity corresponding to the cycloid trajectory, as expressed in Equation 3.22.

$$\begin{aligned}\dot{x}(t_{phase}) &= r1 \cdot 2 \cdot \pi \cdot \text{freq\_swing} \cdot \left(1 - \cos\big(2 \cdot \pi \cdot \text{freq\_swing} \cdot (t_{phase} - t_{0,swing})\big)\right), \\ \dot{z}(t_{phase}) &= r2 \cdot 2 \cdot \pi \cdot \text{freq\_swing} \cdot \sin\big(2 \cdot \pi \cdot \text{freq\_swing} \cdot (t_{phase} - t_{0,swing})\big)\end{aligned} \tag{3.22}$$

Bezier curve Bezier curves are widely used as foot-end trajectories for quadruped robots with advantages, such as simple control, high descriptive power and eased generation for complex smooth curves. The Bezier curve can be expressed as follows [48]:

$$BZ(t) = \sum_{i=0}^{n} \begin{pmatrix} n \\ i \end{pmatrix} t^i (1-t)^{n-i} P_i, \quad 0 \leq t \leq 1, \tag{3.23}$$

where P_i are elements of $\mathbb{R}^k$, $k \leq n$, and called Bezier points [49].

The 2D Bezier curve employed in this implementation is defined by the control points $P_k(x, z)$, where $P_0(0.0, 0.0), P_1(0.08, 0.1), P_2(0.09, 0.1), P_3(0.07, 0.0)$. Subsequently, the desired Bezier Curve for the swinging leg's x and z axes can be computed with respect to frame T_j of the swinging leg j as:

$$\begin{aligned} xBezier(t) &= (1-t)^3 \cdot P_{0,x} + 3 \cdot t \cdot (1-t)^2 \cdot P_{1,x} + 3t^3 \cdot (1-t) \cdot P_{2,x} \\ &\quad + \tau_i^3 \cdot P_{3,x}, \\ zBezier(t) &= (1-t)^3 \cdot P_{0,z} + 3 \cdot t \cdot (1-t)^2 \cdot P_{1,z} + 3t^3 \cdot (1-t) \cdot P_{2,z} \\ &\quad + \tau_i^3 \cdot P_{3,z} \end{aligned} \tag{3.24}$$

Taking the first derivative of the aforementioned equations allows us to calculate the desired tip velocity relative to the frame T_j as follows:

$$\begin{aligned} \dot{x}Bezier(t) &= 3 \cdot (1-t)^2 \cdot (P_{1,x} - P_{0,x}) \\ &\quad + 6 \cdot t \cdot (1-t) \cdot (P_{2,x} - P_{1,x}) + 3t^2 \cdot (P_{3,x} - P_{2,x}), \\ \dot{z}Bezier(t) &= 3 \cdot (1-t)^2 \cdot (P_{1,z} - P_{0,z}) \\ &\quad + 6 \cdot t \cdot (1-t) \cdot (P_{2,z} - P_{1,z}) + 3t^2 \cdot (P_{3,z} - P_{2,z}) \end{aligned} \tag{3.25}$$

Notice that in Equations (3.24) and (3.25), t s not the time but a parameter to introduce time. Then, the above equations are expanded for the desired duration of the swinging leg, as $t \in [0, 1]$. Fig. 3.11 illustrates the desired 2D Bezier curve with respect to the CoM:

Transformation Additionally, we denote the initiation time of a phase concerning the total experiment duration as $t_{0,phase} \in \mathbb{R}$. When a new phase commences at $t_{0,phase}$, we record the position of leg j's tip with respect to the world frame, as

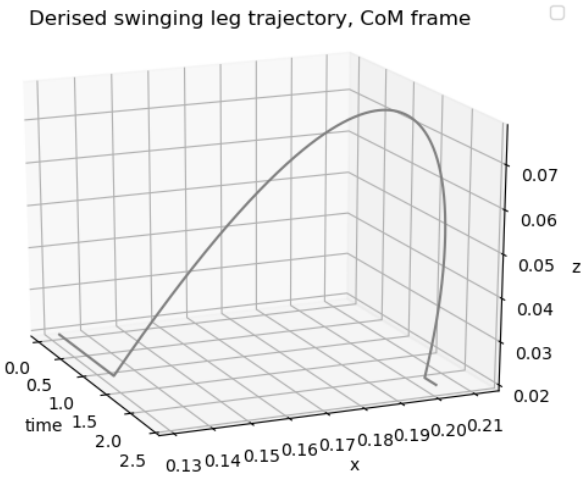

Figure 3.11: Bezier Desired swinging leg trajectory, refer. CoM.

$\mathbf{p0}_j \in \mathbb{R}^3$. This position serves as a reference point for the start of desired swinging trajectory of each phase. In the context of the swinging leg, the previously described desired swinging trajectory and velocity pertain to frame $\{T_j\}$. Frame $\{T_j\}$ is characterized by its position indicated as $\mathbf{p0}_j$ and shares the same axis orientation as the global frame $\{0\}$. To enhance clarity, an example of these frames is depicted in Fig. 3.12. In Fig. 3.12a, we depict frame poses using a realistic representation of the robot model. In contrast, Fig. 3.12b offers a simplified view by superimposing these frame poses onto a bounding box or skeletal structure for enhanced clarity and simplicity.

The desired swinging trajectory vector of the tip j with respect to frame $\{T_j\}$, is called $\mathbf{p}_{d,T_j} \in \mathbb{R}^3$ and accordingly the velocity $\dot{\mathbf{p}}_{d,T_j} \in \mathbb{R}^3$, respectively given by:

in case of cycloid trajectory (3.26) and (3.27):

$$\mathbf{p}_{d,T_j}(t_{phase}) = [x(t_{phase}), 0.0, z(t_{phase})]^\intercal \tag{3.26}$$

$$\dot{\mathbf{p}}_{d,T_j}(t_{phase}) = [\dot{x}(t_{phase}), 0.0, \dot{z}(t_{phase})]^\intercal \tag{3.27}$$

in case of cycloid trajectory (3.28) and (3.29):

$$\mathbf{p}_{d,T_j}(t_{phase}) = [xBezier(t_{phase}), 0.0, zBezier(t_{phase})]^\intercal \tag{3.28}$$

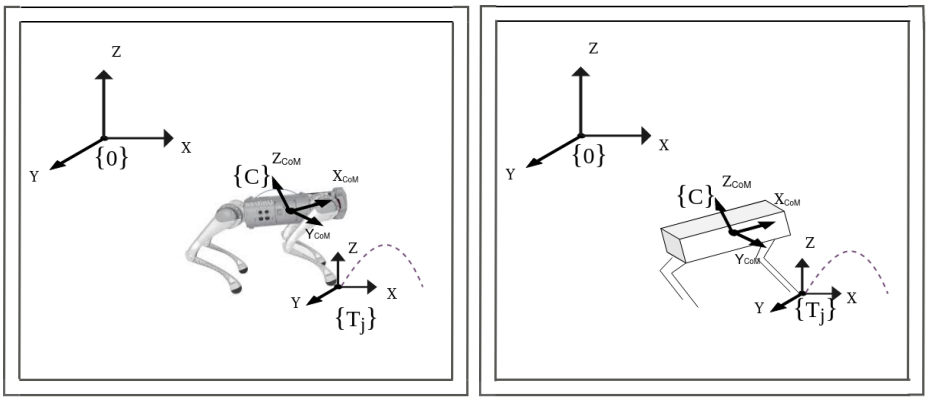

(a) Realistic representation (b) Skeletal structure representation

Figure 3.12: Visualization of Multiple Frame Poses

$$\dot{\mathbf{p}}_{d,T_j}(t_{phase}) = [\dot{x}Bezier(t_{phase}), 0.0, \dot{z}(t_{phase})]^\intercal \tag{3.29}$$

Notice that y axis is 0.0 since the trajectory is about x and z axis only.

As a final step, we can obtain both the desired swinging trajectory and its corresponding desired velocity relative to the $\{C\}$ frame. It's worth noting that this procedure is essential for implementing CLIK, enabling the derivation of the desired joint values, denoted as $\mathbf{q}$, for each joint, effectively transitioning from task space to joint space.

Then, the trajectory with respect to the inertial frame is given by:

$$^0\mathbf{p}_d(t_{phase}) = \mathbf{H} \cdot [\mathbf{p}_{d,T_j}(t_{phase})^{-\intercal}, 1]^\intercal \tag{3.30}$$

,where $^0\mathbf{p}_d(t_{phase}) \in \mathbb{R}^4$ and $\mathbf{H} \in \mathbb{R}^{4\times4}$ is the homogeneous transformation matrix (3.31). Notice, that we extract only the first 3 elements from the vector $^0\mathbf{p}d(tphase) \in \mathbb{R}^4$, as it pertains to a homogeneous transformation.

$$H = \begin{bmatrix} \mathbf{I}_3 & \mathbf{p0}_j \\ 0 & 1 \end{bmatrix} \tag{3.31}$$

Consequently, the desired velocity is also expressed to the respect of world frame, denoted as $0\dot{\mathbf{p}}_d(t_{phase})$.

CLIK CLIK represents a control methodology specifically designed for legged robots. CLIK combines the principles of compliance and inverse kinematics to orchestrate precise and adaptable leg movements. This approach serves as a pivotal link between high-level trajectory planning and the nitty-gritty details of

joint control. By infusing compliance into the control framework, CLIK equips legged robots with the ability to not only follow predetermined trajectories with precision but also gracefully adapt to varying terrains and external disturbances. This adaptability is essential for achieving stable locomotion and executing agile maneuvers in challenging real-world environments.

As we possess a predefined trajectory for the end-effector of the swinging leg j, our objective is to implement a mechanism to ensure its adherence to this trajectory. For this purpose, we have opted for the CLIK approach to govern the tip's behavior in joint space. CLIK's seamless integration into the control framework allows us to bridge the gap between trajectory planning and precise leg control, enhancing our robot's ability to execute tasks with both accuracy and compliance.

The CLIK equation is presented as follows in Equation 3.32:

$$\dot{\mathbf{q}} = \mathbf{J}_j^{-1} \cdot (\dot{\mathbf{p}}_{d,C,j} - k_{clik} \cdot (\mathbf{p}_{c,j} - \mathbf{p}_{d,C,j})) \tag{3.32}$$

where, $\mathbf{J}_j^{-1} \in \mathbb{R}^{3\times3}$ represents the inverse Jacobian matrix pertaining to the selected leg indexed as j, and $\mathbf{p}_{c,j}$ denotes the position vector of the tip of leg j relative to the frame of the CoM, which is denoted as C.

To further elucidate, let $\dot{\mathbf{p}}_{d,C,j}$ and $\mathbf{p}_{d,C,j}$ denote the desired velocity and position, respectively, for the desired swinging trajectory of the swinging leg. These values are expressed in the CoM frame C.

The output of the CLIK process, as given by Equation 3.32, provide us with a joint velocity vector $\dot{\mathbf{q}}$, which corresponds to the velocity of the swinging leg's tip. By utilizing Euler integration, we yield the joint position commands for the swinging leg at discrete time intervals dt:

$$\mathbf{q}_{k+1} = \mathbf{q}_k + \dot{\mathbf{q}} \cdot dt \tag{3.33}$$

This process enables us to derive the trajectory of the swinging leg based on the desired position and velocity in the CoM frame, leveraging the inverse Jacobian matrix associated with the chosen leg.

Subsequently, we initiate a position control mechanism for the swinging tip j, transmitting exclusively the q values associated with that specific tip. Meanwhile, the remaining three legs receive their command signals based on the computed torque of control efforts, a critical step aimed at preserving the robot's stability and equilibrium during its motion.

3.4.1.3 Accomplishing free gait

In the context of assessing and triggering locomotion in this study, building upon the backdrop of agile movements, we introduce a notable locomotion pattern known as free gait. The adoption of accomplishing free gait in this context carries a multitude of advantages and merits that are worth highlighting and exploring further. We opted for the free gait pattern to assess the performance of our proposed body movement controller in the context of free gait locomotion. As part of potential

future work, we can explore the integration of environmental sensors, such as terrain maps, to enable adaptive locomotion tailored to the specific environmental conditions.

i) **Terrain Adaptability:** Free gait excels in adapting to diverse terrains by utilizing real-time adjustments in leg movements and body posture. This adaptability allows the robot to conform to the specific demands of the terrain it encounters. For example, on rough or uneven terrain, free gait can modify leg movements to ensure stable locomotion, while on flat surfaces, it can optimize for efficiency.

ii) **Obstacle Handling:** Free gait's key feature is its ability to dynamically adjust leg movements and body posture in response to obstacles. When the robot encounters an obstacle, it can autonomously adapt its gait to step over, around, or even onto the obstacle. This flexibility in obstacle negotiation ensures that the robot can navigate complex environments with agility and precision.

iii) **Energy Efficiency:** Free gait optimizes energy usage by tailoring its gait patterns to the specific requirements of the task. For instance, when traversing flat and even terrain, it can adopt a more energy-efficient gait pattern. However, when facing steep inclines or rough terrain, it can adjust its gait for stability and performance. This adaptability ensures efficient energy utilization.

iv) **Dynamic Stability:** Free gait provides dynamic stability through real-time adjustments. When the robot encounters disturbances, such as unexpected terrain variations or external forces, it can swiftly adapt its leg movements and body posture to maintain balance. This dynamic response minimizes the risk of falls and ensures the robot remains stable in challenging situations.

v) **Gait Variability:** Unlike fixed gaits that are rigid and predefined, Free gait offers a high degree of flexibility in selecting and adapting gait patterns. This flexibility allows the robot to choose the most suitable gait for the current situation. For example, it can switch between walking, trotting, or even crawling gaits, optimizing its performance and adaptability based on task requirements.

vi) **Sensor Integration:** Free gait is designed with the flexibility to incorporate advanced sensors seamlessly. These sensors provide real-time environmental feedback, such as terrain roughness or obstacle detection. By integrating this sensor data into its control algorithms, Free gait can make informed decisions, adjust its gait, and respond intelligently to its surroundings.

vii) **Versatile Applications:** Free gait's adaptability and agility make it suitable for a wide range of applications. In agriculture, it can navigate crop fields

with ease. In exploration, it can traverse challenging terrains, including rocky landscapes or uneven surfaces. In surveillance, it can negotiate obstacles during patrols. In disaster response, it can reach disaster-stricken areas efficiently. Its versatility allows it to excel in diverse tasks and environments, making it a valuable choice for various applications.

The array of benefits associated with free gait position it as a versatile and promising locomotion strategy that suits a variety of scenarios. The choice to employ free gait, even in an early stage, in this specific context aligns with its aptness for navigating demanding terrains and challenging environments for future work.

In the general process of moving forward using free gait, a quadruped can follow the straightforward sequence :

a) **Initial Stance:** All four legs are initially in contact with the ground, providing stability.

b) **Leg Selection:** The quadruped selects one of its raised legs to begin the movement. For instance, the front-right leg.

c) **Swing and Land:** The chosen leg goes through a swinging motion, lifting off the ground and then landing in a position that supports forward motion.

d) **Weight Transfer:** As the leg lands, the quadruped shifts its weight onto this leg, slightly lifting one of the previously supporting legs.

e) **Repeat and Rotate:** The quadruped repeats this process by selecting and moving a different leg. This rotation ensures that only one leg moves at a time while the others provide stability.

f) **Continuous Motion:** By continually selecting and moving legs in a coordinated manner, the quadruped achieves forward movement while maintaining balance.

This straightforward approach allows the quadruped to move forward without adhering to a specific gait pattern. It's a simple yet effective method adaptable to various terrains and scenarios.

In this study, we've adopted the following leg sequence: (1.) Front-Right (FR), (2.) Rear-Left (RL), (3.) Front-Left (FL), (4.) Rear-Right (RR). The locomotion cycle is structured into four distinct phases, each corresponding to the selection of one of these legs (FR, RL, FL, RR). In the context of our research, we define "Phase j" as the combined stance and swing phase of leg j. To provide a clearer understanding of this locomotion pattern across one complete cycle, the forthcoming diagrams will illustrate it comprehensively.

In each "Phase j" of locomotion, the sequence of swinging legs follows the predetermined order we established earlier. Consequently, we calculate the updated

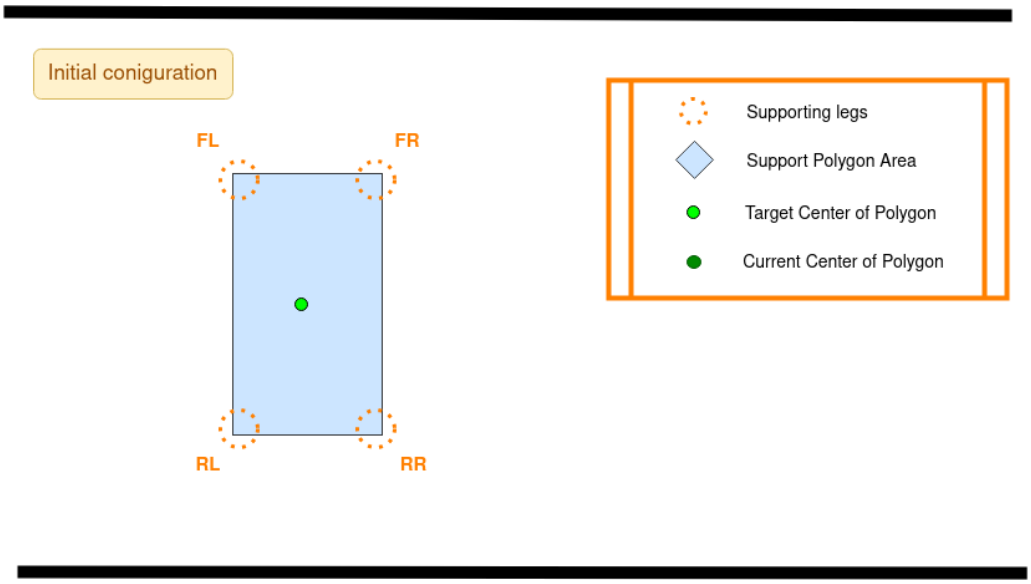

Figure 3.13: Initial configuration of Locomotion

center of the Support Polygon for the ongoing "Phase j" as our target. This recalculated center of Support Polygon then acts as an attractor for the CoM under the control of the Body Movement controller. Over time, since we have adapted the weights of the swinging leg j, $w_{j,0}, w_{j,1}, w_{j,2}$, the swinging leg executes the prescribed swinging trajectory, and we gradually approach the target configuration, preparing for the subsequent phase to advance our locomotion process. Figure 3.13 illustrates the initial configuration prior to the commencement of locomotion. Subsequently, Figures 3.14, 3.15, 3.16, and 3.17 depict the sequential progression through each of the four phases within a single locomotion cycle.

In Phase 0, we designate the FR leg as the swinging leg. The objective is to align the projection of the CoM with the center of the support polygon, while excluding the FR leg as a contact point. Throughout the stance phase, the CoM is directed towards this target, as depicted in the left section of Figure 3.14 and the support polygon is indicated by the blue-shaded area on the right side of Figure 3.14.

During Phase 1, the RL leg takes on the role of the swinging leg. The support polygon comprises the contact points of the FR, FL, and RR legs, excluding the RL leg. The process for guiding the CoM to the target and subsequently swinging the RL leg remains the same, Fig. 3.15.

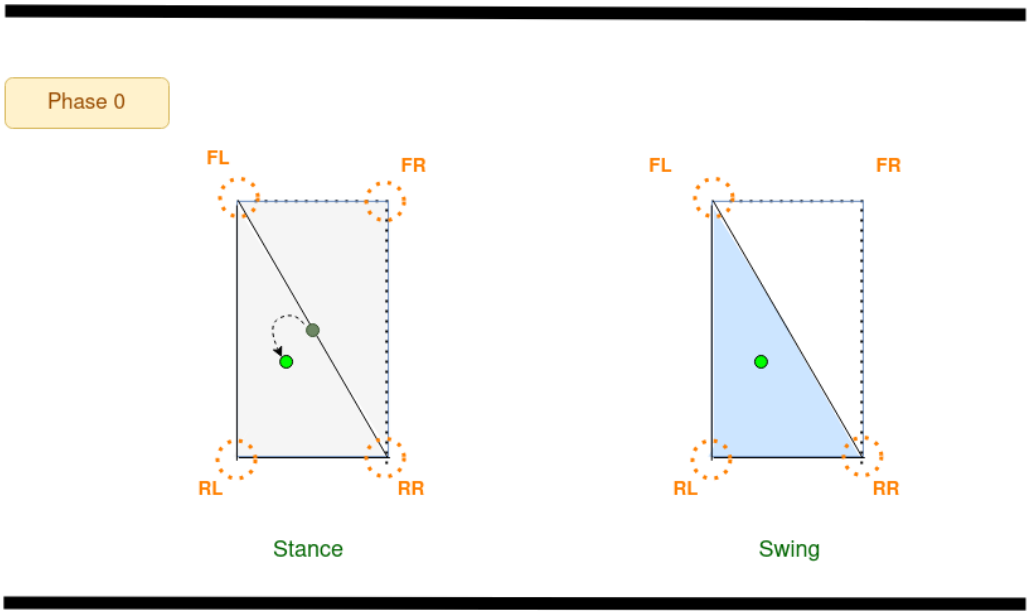

Figure 3.14: Phase 0

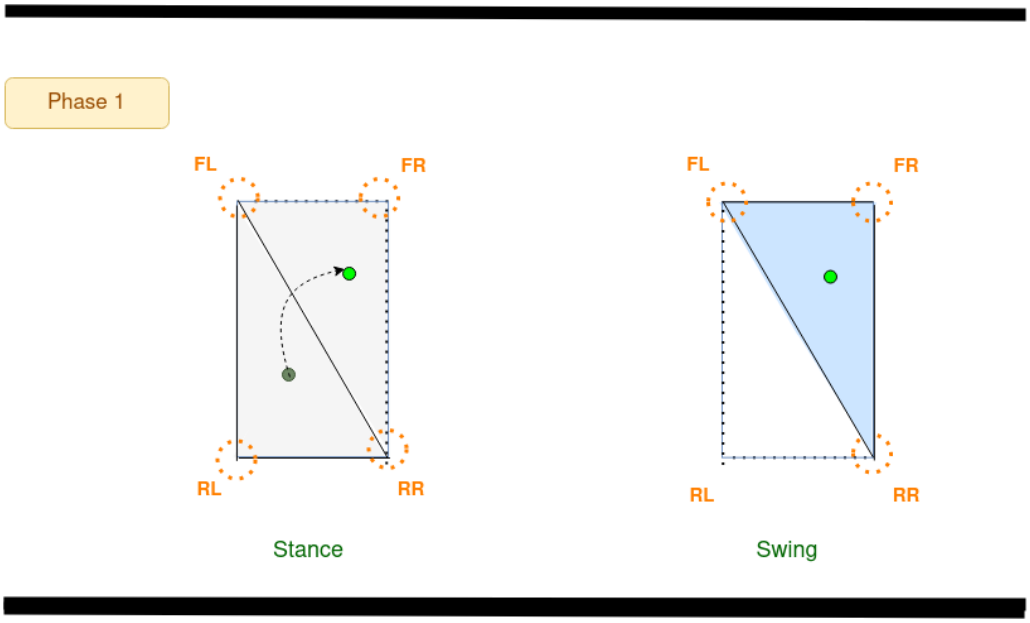

Figure 3.15: Phase 1

During Phase 2, illustrated in Fig. 3.16, the FL leg becomes the swinging leg, while the remaining legs provide support through effort control.

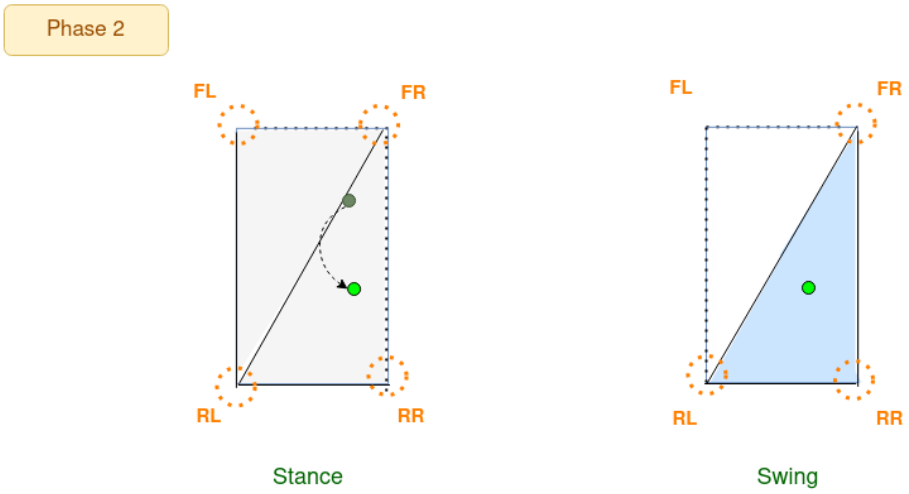

Figure 3.16: Phase 2

In the last phase for a single locomotion cycle, Phase 3, as Fig. 3.17 presents, the RR leg is the swinging leg.

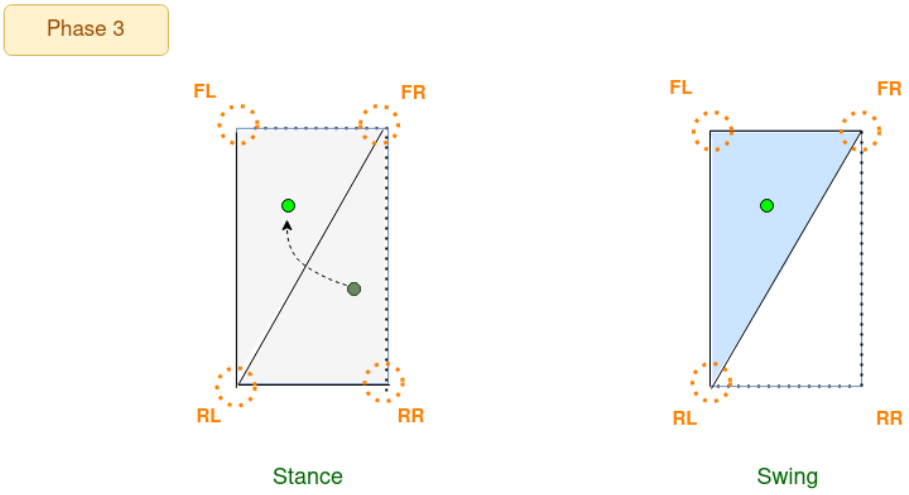

Figure 3.17: Phase 3

3.4.1.4 Slip detection during locomotion

So far, we have introduced the adaptive Body Movement controller, which employs a unified conceptual approach involving the weighted pseudo-inverse, denoted as $\mathbf{G}^{\dagger}$ (3.7) by adaptive the weights $w_{j,m} \quad m \in 1, 2, 3$ of the j-th swinging leg to a significant high value, for locomotion. This approach enables the controller to simultaneously achieve target reaching and execute desired tasks, such as swinging leg. What is more, the slip detection method described in Section 3.3.2 can be seamlessly integrated into this controller in order to detect if a foot slips during locomotion. To elaborate further, the first layer of adaptation can be adjusted during the locomotion phase while the robot is in the process of reaching its target. It's worth noting that the input for slippage probability from Equation (3.12) is considered for all legs, so $\forall i = 1, ..., 4 \quad$, with $i \neq j$ where j is the swinging leg.

So one can adjust the block diagram of the proposed scheme of the adaptive Body Movement controller in case of slip detection in enabled to:

Ultimately, one can find the comprehensive algorithm for the Body Movement controller presented in Algorithm 2.

Algorithm 2 Implementation of the control loop - Body Movement

Select values for: $k_p, k_o, k_i, \mathbf{K}_v, w_0, w_{max}, \text{freq}_{swing}, t_{\text{half}}$
$\mathbf{W} := w_0 \mathbf{I}_{12}$ ▷ Initialization
Phase:= "Target", $t_{phase} := 0$ ▷ Control phase
while control is enabled **do**
    Get current state of the robot $\mathbf{p}_c, \mathbf{R}_c, \dot{\mathbf{p}}_c, \boldsymbol{\omega}_c$
    if $t_{phase} > t_{swing}$ **then**
        Phase:="Target" ▷ End of current swinging phase
    end if
    switch Phase **do**
        case "Target"
            Select next j-th as swinging leg ▷ Free gait sequence
            $p_T \leftarrow$ center of SP ▷ New target
            $t_{phase} := 0$ ▷ Reset phase time
            Phase:="Swing" ▷ Change state
        case "Swing"
            if Slip detection is enabled **then**
                Estimate $P_i, \forall i = 1, ..., 4 \quad i \neq j$ ▷ Slip. prob. estimator
                Compute $\dot{w}_{i,1}, \dot{w}_{i,2}, \forall i = 1, ..., 4$ from (3.12)
                Integrate $\dot{w}_{i,1}, \dot{w}_{i,2}, \forall i = 1, ..., 4$ to update $\mathbf{W}$
            end if
            Compute $w_{j,m}$ for $m = 1, 2, 3$ from(3.20), update $\mathbf{W}$
            Compute $\mathbf{F}_c$ from (3.16)
            Compute $\mathbf{F}_a$ (includes the $\mathbf{f}_i$-s) from (3.6), (3.7)
            Compute $\boldsymbol{\tau}_i, \forall i = 1, ..., 4$ from (3.4)
            Command $\boldsymbol{\tau}_i, \forall i = 1, ..., 4$ to the joints
            Compute $\mathbf{q}$ from (3.33) for the j-th leg's joints
            Command $\mathbf{q}$ to the j-th leg's joints
end while

3.4.2 Conclusion

In this work, we propose an adaptive "Body Posture and Movement" controller, explained in two different sections. The Body Posture controller is an adaptive trajectory tracking controller which is proposed for quadruped robots and it involves two prioritized layers of adaptation for minimizing the slippage of one or multiple legs. The first adaptation layer considers the dynamic distribution of the control effort among the legs, given the slippage probability for each leg. The second layer, which is enabled only if the problem cannot be solved by the dynamic distribution of the effort, which may occur when all four legs slip, acts on the time-scaling of the trajectory by dynamically and smoothly slowing down the motion, without affecting the spatial properties of the task. The "Body Posture" proposed method is proven to be asymptotically stable. The "Body Movement" controller is characterized as an adaptive controller primarily focused on target-reaching tasks. It shares a common conceptual foundation with the adaptive "Body Posture" controller, employing the adjustment of weights for the swinging leg to facilitate the onset of locomotion within the framework of an accomplished free gait pattern. Additionally, it offers a notable advantage by incorporating slip detection and recovery during locomotion. This capability harnesses the first layer of adaptation from the previously mentioned adaptive "Body Posture" controller, facilitating the dynamic allocation of control effort among the robot's supporting legs.

Chapter 4

Experimental Results

An extensive series of experimental evaluations has been conducted to thoroughly assess the efficacy of the proposed adaptive BPMC across a wide range of scenarios. These assessments encompass both simulated and real-world settings, employing the Unitree's GO1 quadruped robot as the primary test platform (as depicted in Fig. 4.1). Within this chapter, we will delve into a comprehensive presentation of the results obtained through the utilization of the adaptive BPMC. These results are categorized into two distinct sections, each addressing a crucial aspect of the controller's performance. Section 4.1 provides a detailed analysis of the "Body Posture" controller's outcomes, while Section 4.2 delves into the results pertaining to the "Body Movement" controller. The segregation of results allows for a comprehensive examination of the BPMC's performance under various conditions, encompassing both simulated studies and real-world experiments.

4.1 Adaptive Body Posture Control

4.1.1 Simulation Study

To assess the performance of the proposed adaptive "Body Posture" control scheme, we consider five simulation scenarios: a) a simple point-to-point motion to evaluate the trajectory tracking performance, b) a scenario involving the tracking of a periodic motion with the rear right foot contacting a slippery surface, c) a scenario involving the tracking of a periodic motion with global slippage, i.e. all four legs are contacting a slippery surface, d) a scenario in which one foot contacts a slippery surface and another foot is lifted to initiate walking and e) simulations of different terrain type conditions. For the simulations, the model of a Unitree Go1 robot is utilized in the Gazebo environment, right part of Fig. 4.1, and a control cycle of 2ms is considered. The parameters utilized are $k_p = 3000, k_o = 15, \mathbf{K}_v = \text{diag}(550\mathbf{I}_3, 55\mathbf{I}_3), w_0 = 35, \alpha = 150$.

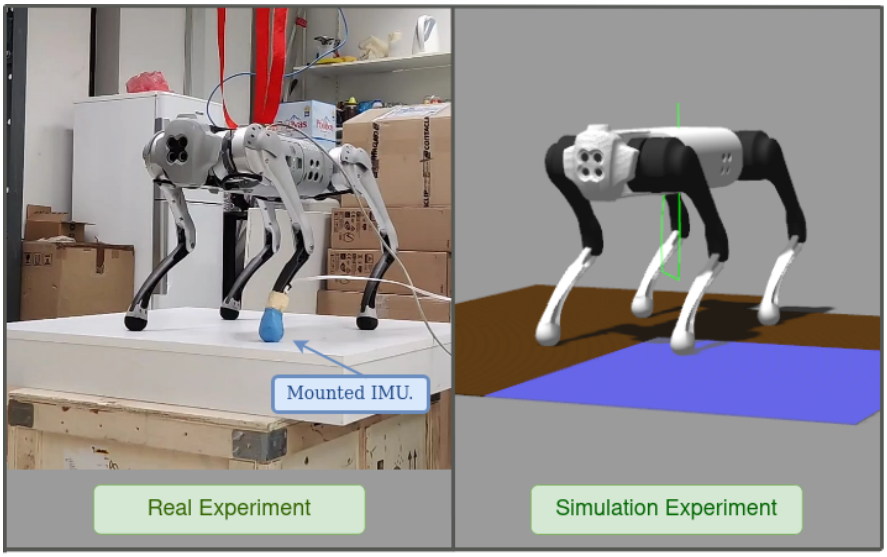

Figure 4.1: The initial configuration of the real and simulation experiments when the front left foot slips. Blue area of the simulation part represents the slippery surface.

4.1.1.1 Scenario 1: Point to point motion

For this scenario, a terrain with a static friction coefficient of 1.4 is considered, representing a non-slippery terrain. The desired trajectory is generated online by the following first order dynamical system: $\dot{\mathbf{p}}_d(t) = \mathbf{p}_d(t) - \mathbf{p}_T$, with $\mathbf{p}_T = \mathbf{p}_d(0) + [0.1\ 0.05\ -0,005]^\intercal$ being the constant target. The initial actual and desired values are $\mathbf{p}(0) = [-0.043\ -0.0037\ 0.356]^\intercal$m and $\mathbf{p}_d(0) = [-0.023\ 0.0063\ 0.355]^\intercal$m in order to impose an initial position error of $\mathbf{e}_p = [-2\ -1\ 0.1]^\intercal$cm. In Fig. 4.2 the actual position evolution is compared to the desired trajectory, in which one can notice the tracking performance. Notice that the tracking performance is affected by the unmodelled joint friction that acts as a disturbance to the system, with the z-direction being the most disturbed direction, due to the manipulability ellipsoid of the given robot's configuration. One could possibly reduce this steady state error by further tuning the control gains (as no extensive tuning was performed), or by incorporating an additional integral term to the controller.

4.1.1.2 Scenario 2: One-foot slippage

For the second scenario, the rear right foot of the robot ($i = 3$) is considered to contact a slippery surface having a static friction coefficient of 0.4, which is considered to be unknown for the controller. For the rest of the feet a non-slippery surface is considered. For comparison, two tests are performed, namely one with the adaptive mechanism and the other without it. The desired trajectory involves a periodic sinusoidal motion, executing an ellipse on the $x - z$ plane, for position

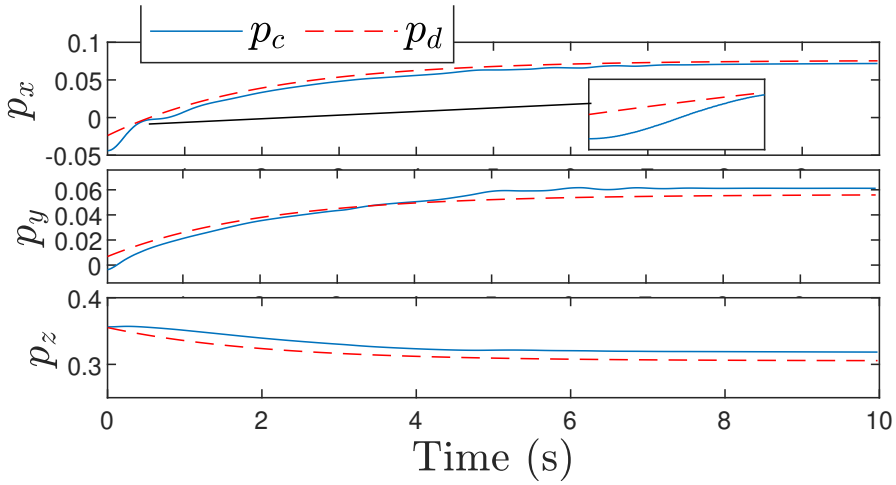

Figure 4.2: [Scenario 1: Point-to-point motion] Time evolution of the actual and desired position.

and a periodic rotation around the x-axis for orientation. The frequency of the periodic trajectory is 0.7Hz and 0.2Hz in position and orientation respectively. The weights of distribution along the x direction of each leg (which is equal to the ones along the y direction), i.e. $w_{i,1}$, are depicted in Fig. 4.3, alongside with the slippage probability provided by the estimator, i.e. $1 - P_i$. Notice the rise of the value of $w_{3,1}$ (the leg that slips), which results in appending less force along the $x - y$ directions of the third leg. Further notice that the third leg stops slipping after the adaptation which means that the force converged to a value within the friction cone and the system reaches a stable steady-state condition.

In Fig. 4.4, the position and orientation errors are depicted, with and without the proposed adaptive scheme for comparison purposes. Notice that without the proposed adaptation mechanism, the system is not able to maintain its stability, as the robot loses contact with the environment at $t \approx 4.5$s. Last, notice that $\beta = 1$ during the whole simulation, due to equation (3.13) and the fact that $w_{i,1} = 35, \forall i = 1, 2, 4$, which means that the first adaptation layer can sufficiently provide a solution by dynamically distributing the control effort.

4.1.1.3 Scenario 3: Global slippage

For this scenario, all four legs of the robot are considered to contact the slippery surface having a static friction coefficient of 0.4. For comparison, we performed two tests, namely one with the adaptive control scheme and one without it and the same trajectory with that of the second scenario is considered. The weights of distribution along the x direction of each leg (which is equal to the ones along the y direction), i.e. $w_{i,1}$, as well as the time-scaling parameter $\beta(t)$ are depicted in Fig. 4.5, alongside with the stable contact probability provided from the estimator,

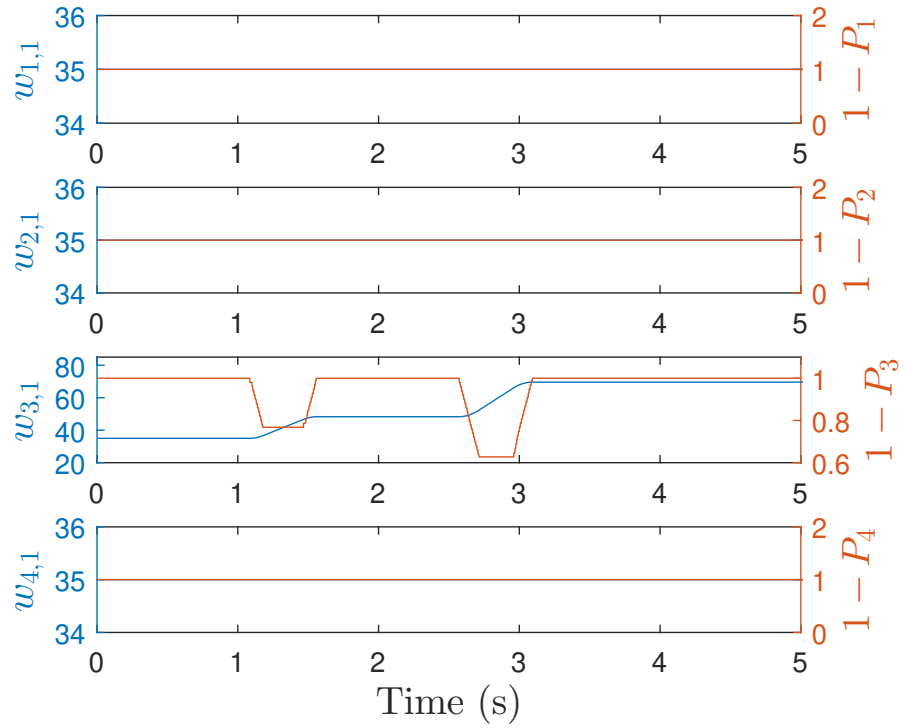

Figure 4.3: [Scenario 2: One-foot slippage] Weight adaptation due to the first layer (the second layer is not enabled).

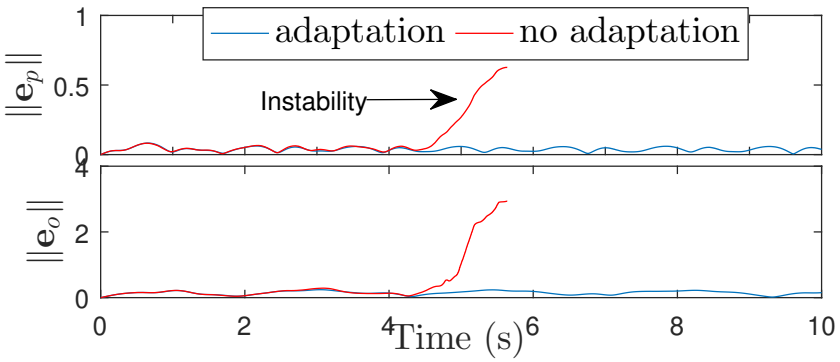

Figure 4.4: [Scenario 2: One-foot slippage] Position and orientation error norms with and without adaptation.

i.e. $1 - P_i$. Notice the rise of the values of all $w_{i,1}$, $i = 1, ..., 4$, which results in slowing down the motion, which is reflected by the reduction of $\beta(t)$ which converges to the value of $\beta \approx 0.77$ after $t \approx 5$s. In Fig. 4.6, the evolution of the position of the CoM in time is depicted both with and without the proposed control scheme.

Notice that without the proposed adaptation mechanism, the system is, also in this case, not able to maintain the stability of the system as the robot, signified by the drop of the CoM in Fig. 4.6. Last, notice the smooth online time-scaling of the trajectory occurred after $t \approx 5$s.

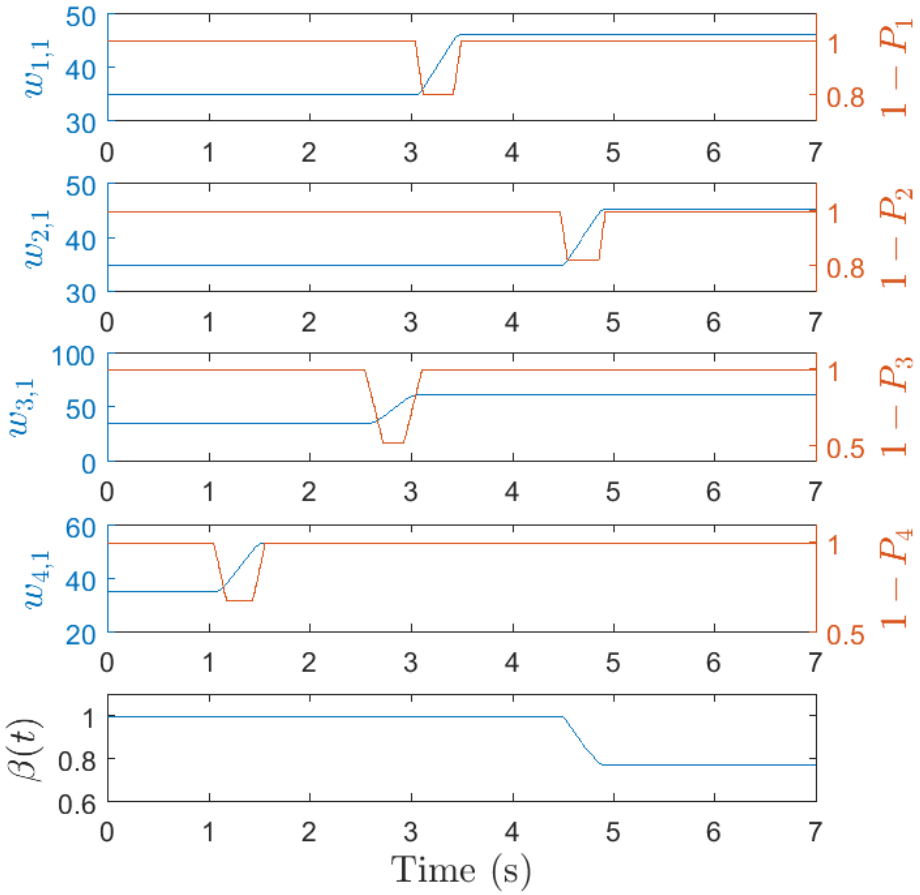

Figure 4.5: [Scenario 3: Global slippage] Weight adaptation due to the first and second layer.

4.1.2 Scenario 4: Elevation of the right-front foot

For this scenario, the rear right foot of the robot is considered to contact the slippery surface (similarly to the second case), while the front right leg is deliberately lifted at $t = 3$s, in order to potentially initiate a walking procedure. The weights of distribution along the x direction of each leg, i.e. $w_{i,1}$, alongside with the stable contact probability provided from the estimator, as well as the norm of the position

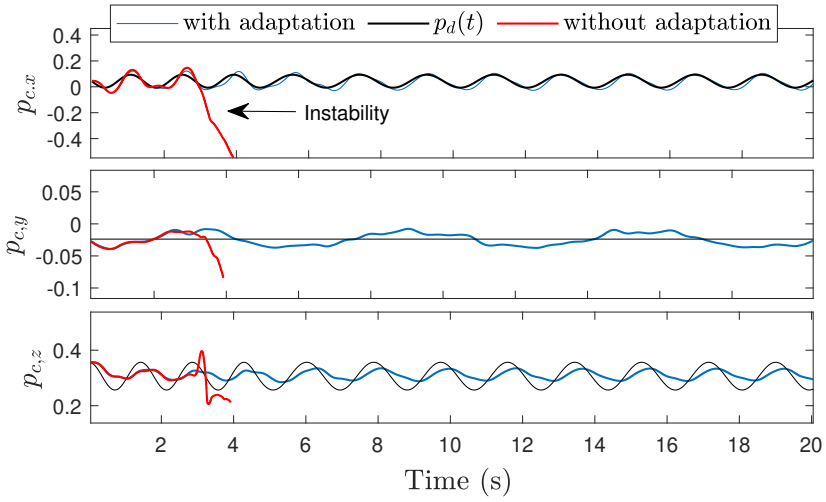

Figure 4.6: [Scenario 3: Global slippage] Evolution of the position of the CoM in time, with and without adaptation.

error are depicted in Fig. 4.7, with and without adaptation. For the motion of the swinging leg, a simple joint-space trajectory is designed, which is followed by a simple joint-space PD controller (only for this foot).

Notice the rise of the weight corresponding to the lifted foot, i.e. $w_{1,1}$, which evolves according to (3.14). Further, notice how the weights of the other legs are affected during the contact loss of the rising foot when the adaptation is enabled, which keeps the robot stable, as opposed to the case in which no adaptation is considered.

4.1.2.1 Scenario 5: Testing in different terrain type combinations.

For this experiment, five different combinations of terrain types are tested, i.e. slippery and not-slippery. In particular, the five cases tested involve a slippery terrain for a) all the feet of the robot, b) the three feet, c) the front feet, d) the two diagonal feet and e) only one feet. The maximum deviation among all the feet from the initial point of contact is given for each use-case in Table 4.1, with and without employing the adaptation mechanism proposed in this work. It is clearly shown that the proposed controller is able to maintain stability in any one of the aforementioned use-cases and ensure that the foot-tip will maintain close to the initial contact point.

4.1.3 Experimental Validation

The evaluation of the proposed adaptive controller is performed on a real Unitree Go1 quadrupedal robot. In order to validate the performance of the first layer of the adaptation mechanism , a 6DOF IMU is attached to the second leg of

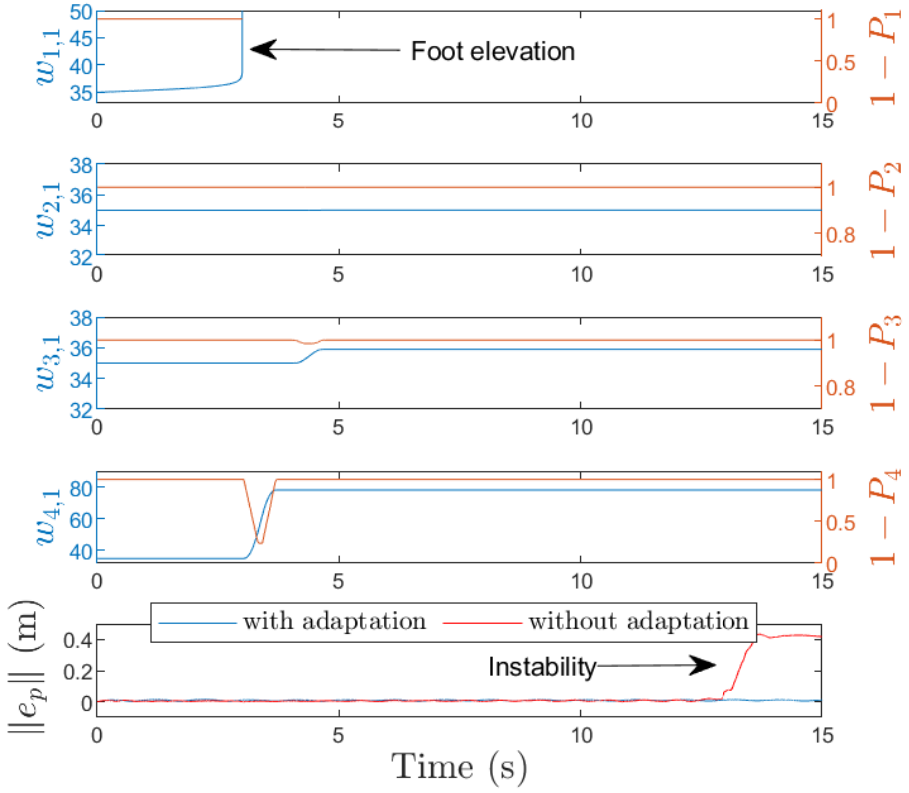

Figure 4.7: [Scenario 4: Elevation of the right-front foot] Weight adaptation during deliberate contact loss.

Table 4.1: Maximum deviation of the foot tips from the initial contact point, i.e. $\max_{\forall i}\left(\max_{\forall t\geq 0}\left(||\mathbf{p}_{ci}(t)-\mathbf{p}_{ci}(0)||\right)\right)$.

Slipping feet	No adaptation*	Proposed*
All	0.984m	0.026m
3 feet	1.09m	0.023m
2 front	0.627m	0.048m
2 diagonal	1.032m	0.018m
1 foot	1.055m	0.035m

*Green color indicates a stable operation and red color indicates instability.

the robot, as shown in Fig. 4.1, which is in contact with a slippery surface, (i.e. lubricant is utilized to emulate the slippery area below the second leg), while the pose of the robot is found online via an external camera with an off-the-shelf

visual odometry system[1] and therefore initial robot's pose is considered as the world frame for the experiment. The proposed adaptive scheme parameters are set to $k_p = 2400, k_o = 15, \mathbf{K}_v = \text{diag}(280\mathbf{I}_3, 28\mathbf{I}_3), w_0 = 35, \alpha = 1000$. The robot was commanded to move along the x-axis with a similar to the second simulation periodic trajectory for the axis of motion, having a frequency of 0.4Hz. The left part of Fig. 4.1 depicts the experimental setup with the robot being in the initial configuration, while in Fig. 4.8, the weight corresponding to the $x - y$ directions of the second leg is given, alongside with the slippage probability estimate; the weights of the rest of the legs remained unaltered during the experiment. In Fig. 4.9 the evolution of position in time is depicted utilizing the adaptive scheme and without its utilization, for comparison. Notice that the activation of the first adaptation layer results in maintaining stability, while when executing the same scenario without enabling the adaptation mechanism the robot is not able to maintain stability at $t \approx 14.6$s. Further, notice that without the adaptation mechanism the tracking performance is affected by the slippage of the second leg, as it triggers unmodelled dynamics.

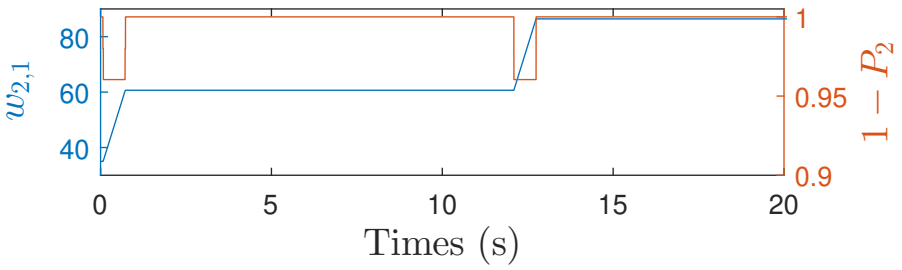

Figure 4.8: The second weight during the experimental validation.

[1] https://github.com/IntelRealSense/librealsense/blob/master/doc/t265.md

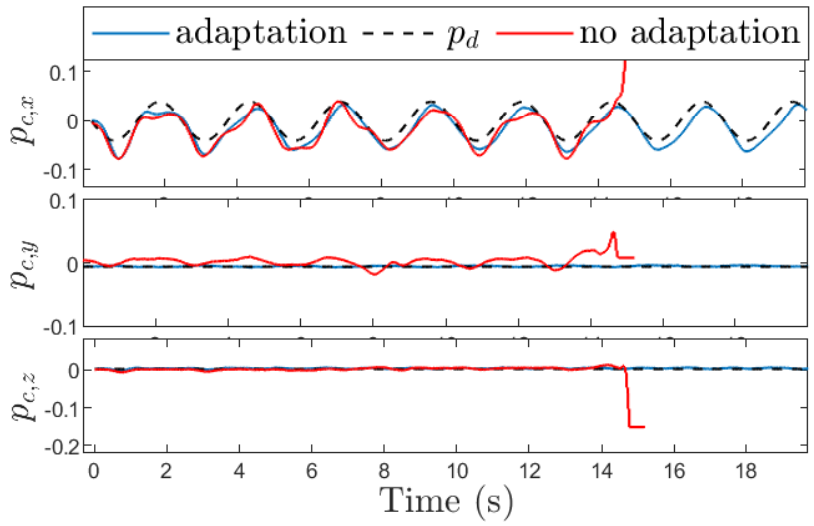

Figure 4.9: Evolution of the position of the CoM in time, with and without adaptation.

4.2 Adaptive Body Movement Control

4.2.1 Simulation

The effectiveness of the adaptive "Body Movement" controller was assessed through testing in two distinct simulated locomotion scenarios utilizing the Unitree GO1 robot within the Gazebo environment. Both scenarios aimed to evaluate the controller's performance during forward locomotion, with each commencing in different types of terrain: (a) a flat, non-slippery surface, and (b) a flat terrain with slippery sections and a cylindrical obstacle. In both scenarios, the results demonstrated the excellent performance of the proposed controller.

In the initial (a) experiment, the "Body Movement" controller demonstrated its capability in successfully executing the locomotion task. In the second (b) experiment, we compared the performance of forward locomotion in slippery and rugged terrains, both with and without adaptation. The findings revealed that without adaptation, the robot would lose balance when it encountered the cylindrical obstacle. However, in the adaptation scenario, where slip detection was activated, the robot successfully identified the slippery surface of the cylinder and, by adjusting its control efforts, effectively overcame the disruptive obstacle.

For each of the upcoming experiments, we specify the parameters as follows. In the Gazebo environment, the control cycle for the Unitree GO1 robot is set to 2 ms. The controller's gain parameters are assigned as follows: $k_p = 1300.0$, $k_o = 15.0$, $k_i = 50.0$, $K_v = \text{diag}(100I_3, 10I_3)$, and $w_0 = 35$. The locomotion design includes parameters such as $freq_{swing} = 1.0$ Hz, $t_{0,swing} = 1.2$ s, and $t_{swing} = 2.5$ s.

Regarding the Super Gaussian, the parameters are defined as follows: $A = 1.0$,

$b = 10.0$, $t_0 = 1.0$ s, and $t_{half} = 1.7$ s. Additionally, the 2D Bezier curve used in this implementation is characterized by control points $P_k(x, z)$, where $P_0(0.0, 0.0)$, $P_1(0.08, 0.1)$, $P_2(0.09, 0.1)$, and $P_3(0.07, 0.0)$ as shown in Figure 3.11.

4.2.1.1 Locomotion in simple terrain

In this simulation scenario, the terrain is characterized as a flat surface devoid of any slippery conditions. The primary objective is to achieve forward locomotion, building upon the "accomplishing free gait" concept introduced in the previous chapter 3.3. It's important to observe that this controller operates with a target-reaching approach, where the target for the CoM changes in every new phase. Figure 4.10 illustrates the current and target positions of the CoM along each axis. It's evident that, by the end of the cycle, the target positions in both the x and y axes are effectively reached. However, it's important to acknowledge that the reaching target performance is influenced by unaccounted joint friction, which serves as a disruptive force in the system. The most notable disruption occurs in the z-direction due to the demands of the locomotion task.

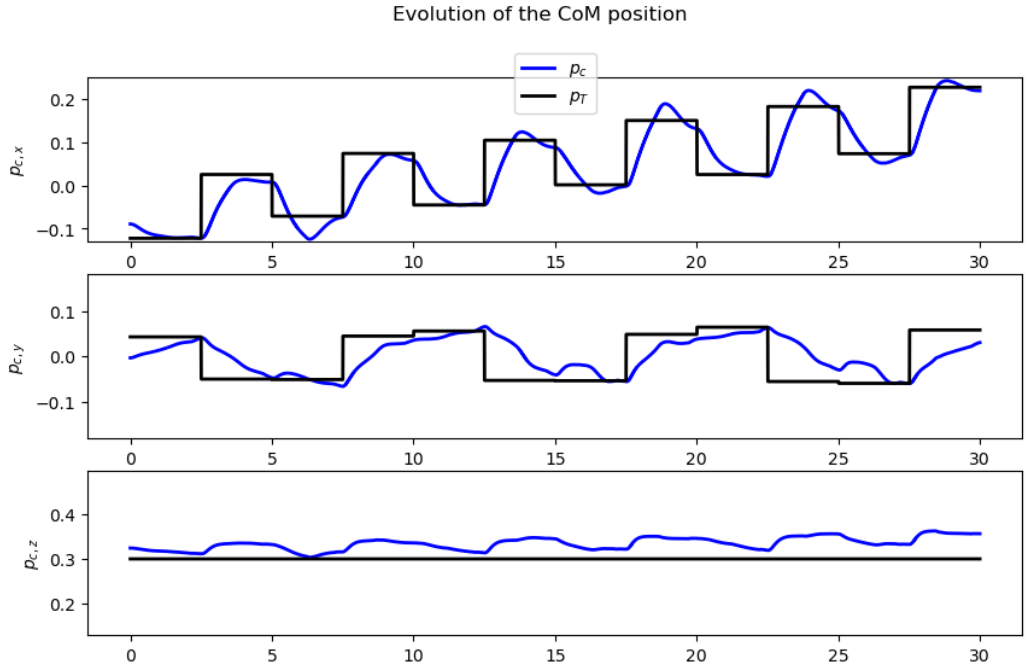

Figure 4.10: Current and target position for each axis of CoM, during forward locomotion.

Figure 4.11 displays the positional error observed during locomotion. Notably, the error pattern exhibits a consistent trend, which aligns with expectations due to the symmetrical nature of the gait. It's evident that higher error values occur each time a new target is established, coinciding with the initiation of a new phase

(indicated by red vertical dots to demarcate phase cycles). Subsequently, the error gradually diminishes and converges towards lower values.

For a more detailed examination of the mentioned performance characteristics, Figure 4.12 presents a zoomed-in version of a specific cycle, allowing for a closer inspection of these behaviors.

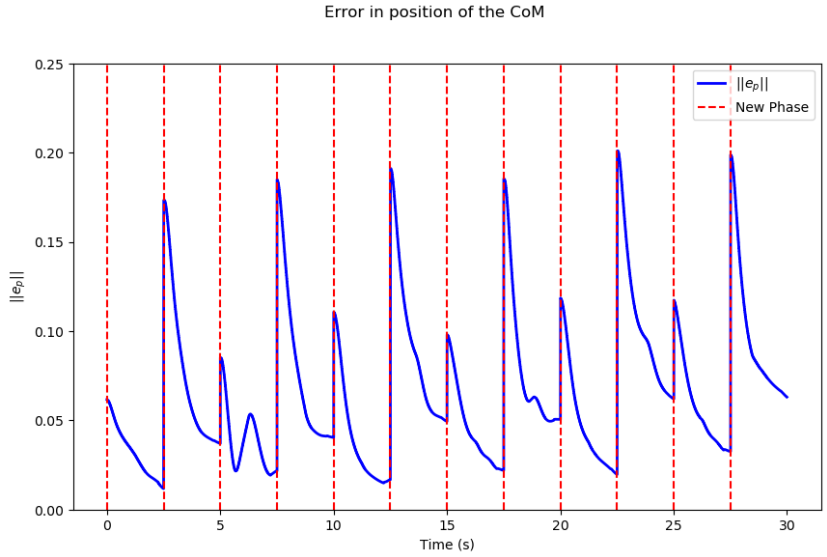

Figure 4.11: Error in position for the CoM, during forward locomotion.

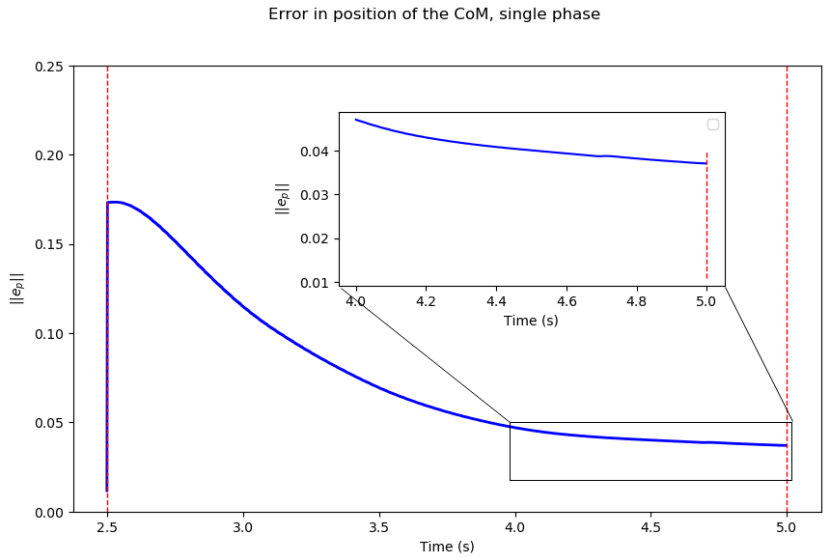

Figure 4.12: Error in position for the CoM, during a single phase in locomotion.

In the context of the locomotion task, our primary focus does not include

the target orientation because it has a relatively minor impact on the overall stability during the initiation of locomotion. Simultaneously, slight adjustments in the robot's orientation are necessary to facilitate the robot's configuration for movement, thereby contributing to its role in free gait locomotion, Fig. 4.15. Figure 4.13 illustrates the orientation performance during locomotion, with an average error measuring 0.044 and a maximum error of 0.10.

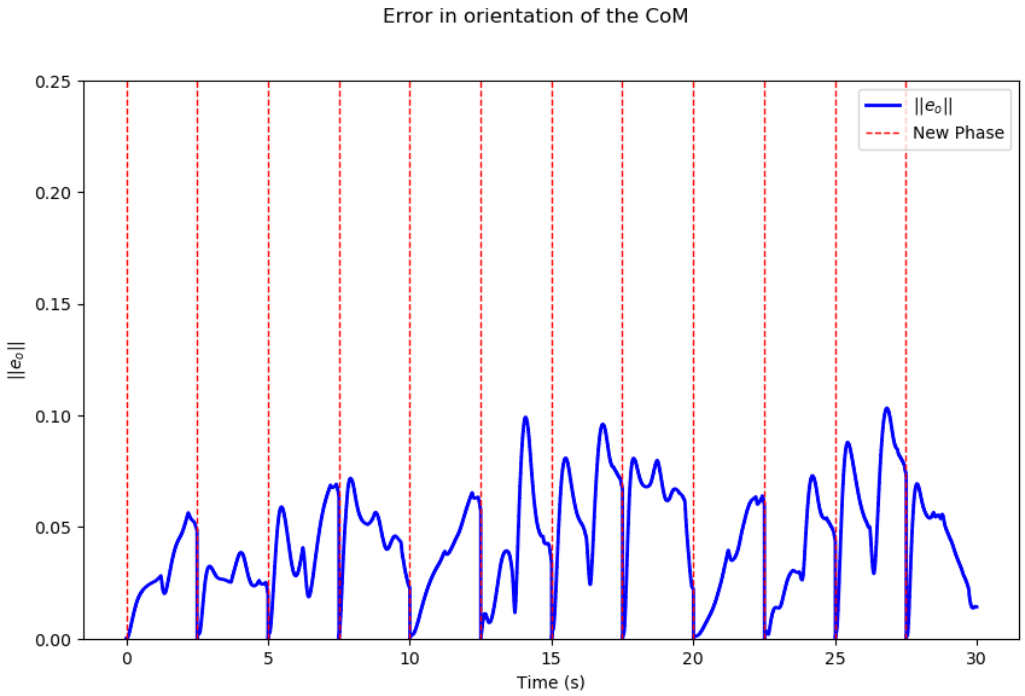

Figure 4.13: Error in orientation for the CoM, during forward locomotion.

Throughout the locomotion study, we have recorded the position of the end-effector relative to the world frame. Figure 4.14 reveals that the controller has effectively demonstrated an exceptional capability in achieving precise end-effector desired tracking for the swinging leg, ensuring that the tip is consistently positioned as intended.

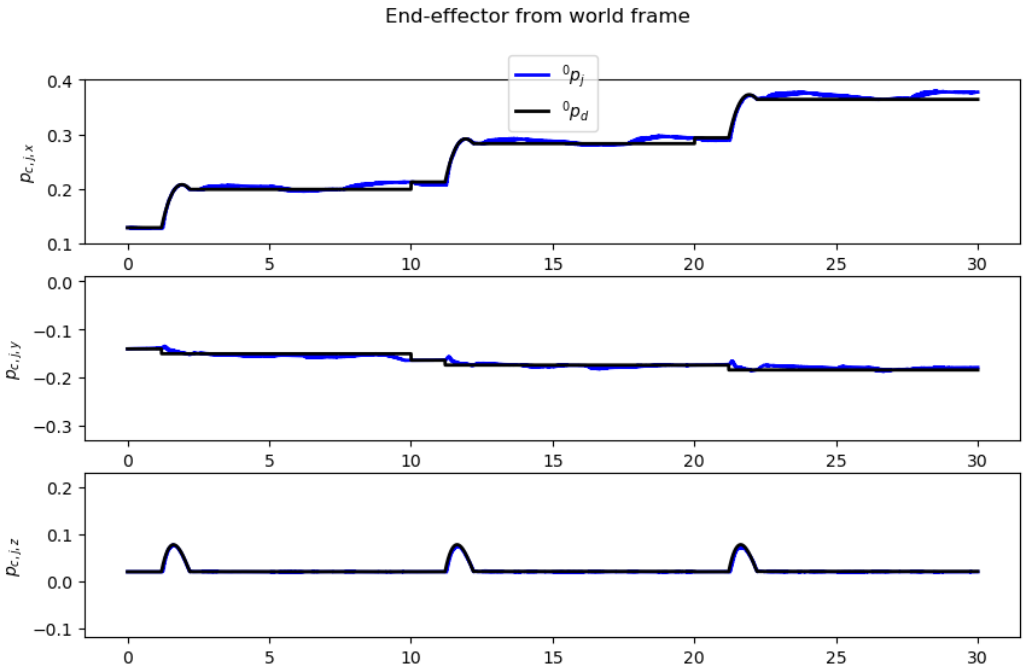

Figure 4.14: End-effector position of FR leg, with respect to 0 frame, during forward locomotion.

4.2.1.2 Adaptive forward movement

The "Body Movement" controller's performance was also assessed in adaptive mode, with slip detection enabled to mitigate potential slippage and maintain the robot's stability. In this experiment, we examine a scenario where the robot lifts its right front (FR) foot to navigate around a cylindrical object, as it is shown in Fig. 4.16. Subsequently, we will compare the controller's performance both with and without the adaptation mechanism.

As demonstrated, the robot experiences a loss of stability when the adaptation mechanism is not in use. However, when the adaptation is enabled, the robot successfully maintains its stability and continues walking. The parameters utilized in this experiment remain consistent with those described in the initial section of this chapter, with the addition of the parameter $\alpha = 150$, needed for the adaptation mechanism.

In Figure 4.17, the position of the CoM along each axis during locomotion is depicted. The red color represents the actual CoM position during locomotion without adaptation, while the gray line corresponds to the target position. It's particularly evident in the z-axis that, as the robot steps onto the cylinder object, it loses contact with the ground and falls.

In contrast, the blue and dark plot, which corresponds to the same variables with the adaptation mechanism in place, effectively maintains the robot's stability

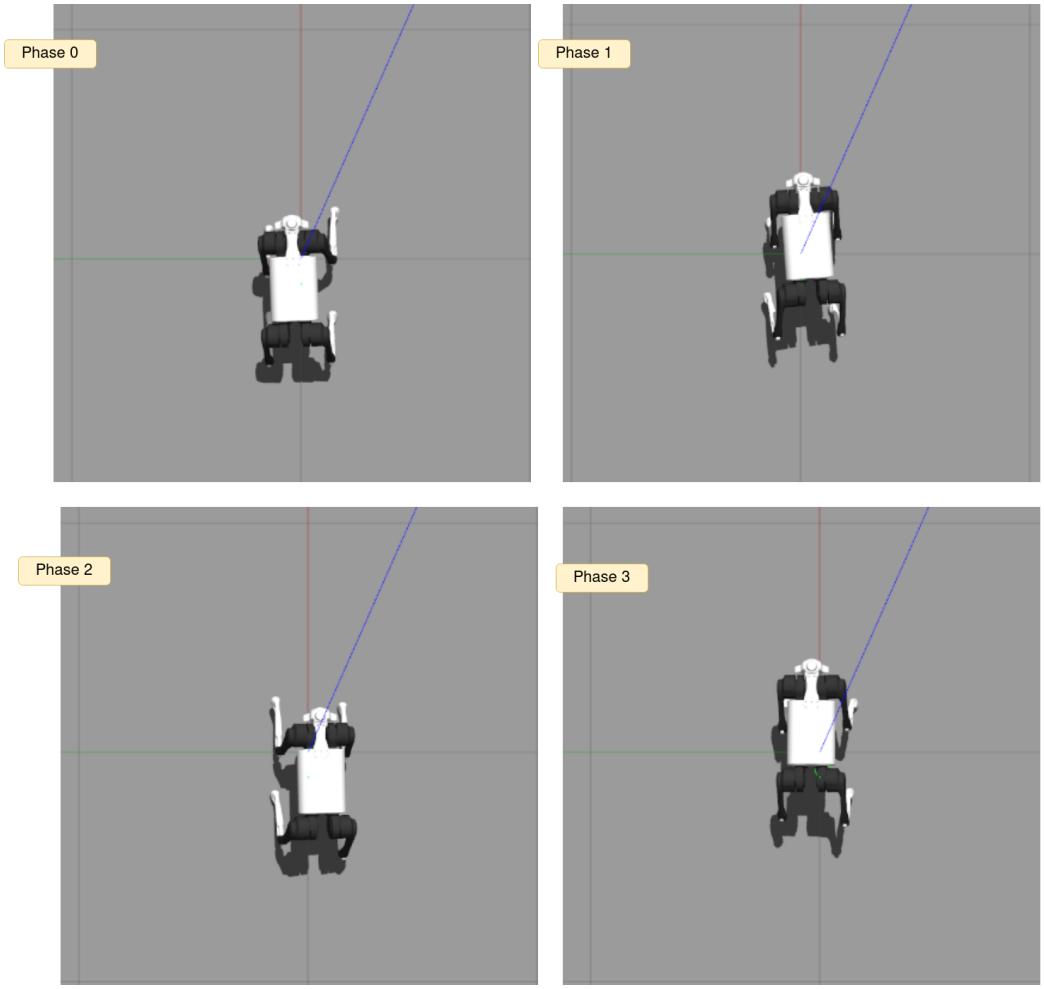

Figure 4.15: Robot configuration in each phase, during one cycle of forward locomotion.

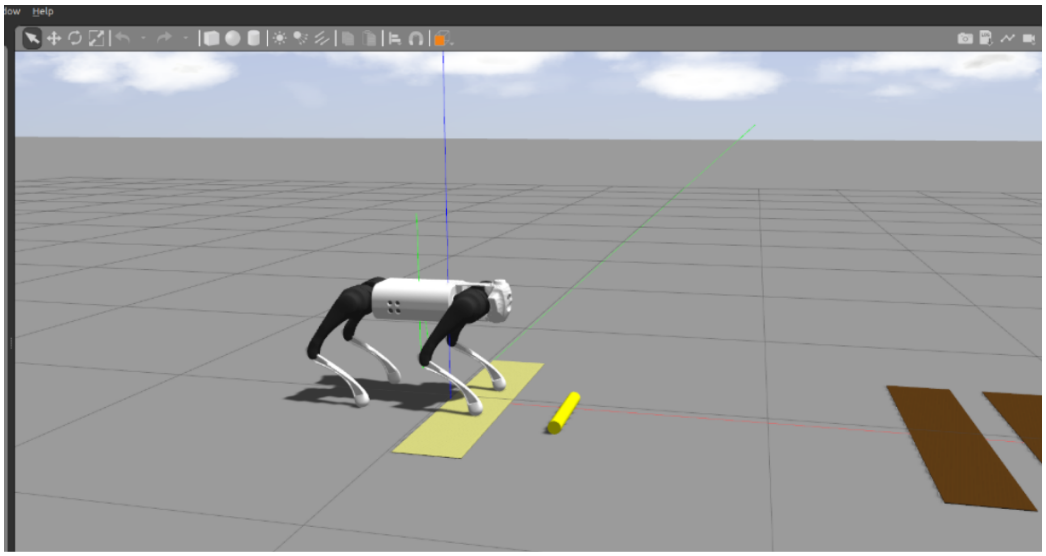

Figure 4.16: Simulation configuration involving a cylinder in Gazebo environment.

without compromising its gait and intended task.

Figures 4.18 and 4.19 provide insight into the errors in position and orientation. As previously explained in the context of the experiment for locomotion in uncomplicated terrains, the error is more pronounced at the beginning of each new phase when the target for the new phase is established. Subsequently, the position error decreases, with exception being the cylinder contact event for the non-adaptive case of the "Body Movement" controller.

Both Figures 4.18 and 4.19 illustrate the loss of control over the robot following the contact of the end-effector with the cylinder object.

In terms of the positioning of the FR leg during this locomotion experiment, the adaptive movement controller, as proposed, effectively maintains the robot's stability and accomplishes the intended task for the end-effector, even in the face of an unforeseen event at $t = 23.5s$. Conversely, the proposed controller without adaptation initially experiences a loss of tip position in the y-axis, and over time, it leads to subsequent deviations in the x and z axes of the FR end-effector at $t = 27.0s$.

Figure 4.21 presents the adaptive weight distribution across each foot. It's important to note that the high-value windows have been configured to allow the swinging leg to effectively manage the desired task, through super Gaussian function.

Furthermore, the smaller values of weight adaptation, indicate that the system is receiving a higher probability of slippage as input. In this regard, the controller effectively maintains stability even in contact events, such as when placing the end-effector against a cylinder.

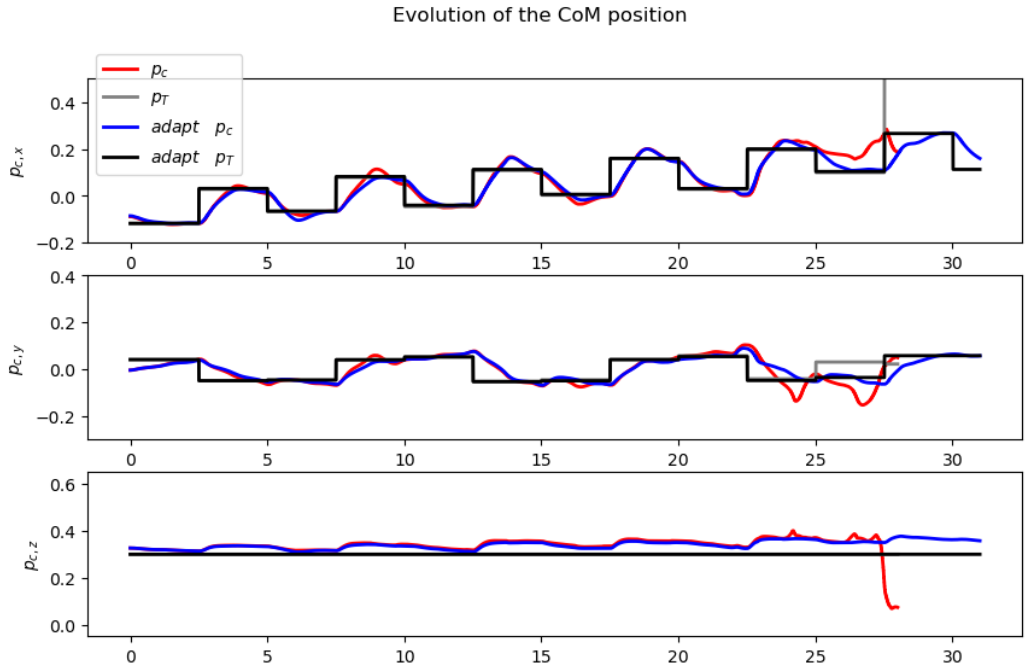

Figure 4.17: Current and target position for each axis of CoM, during adaptive forward locomotion.

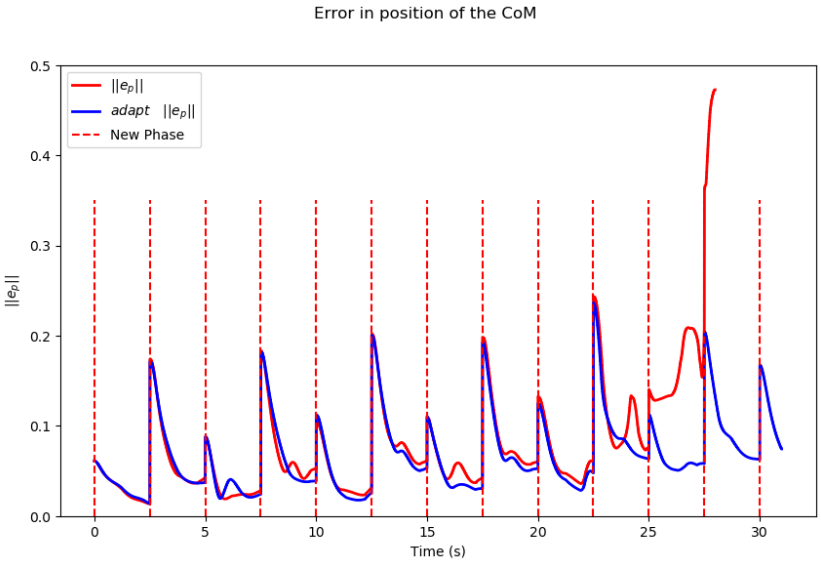

Figure 4.18: Error in position for the CoM, during adaptive forward locomotion.

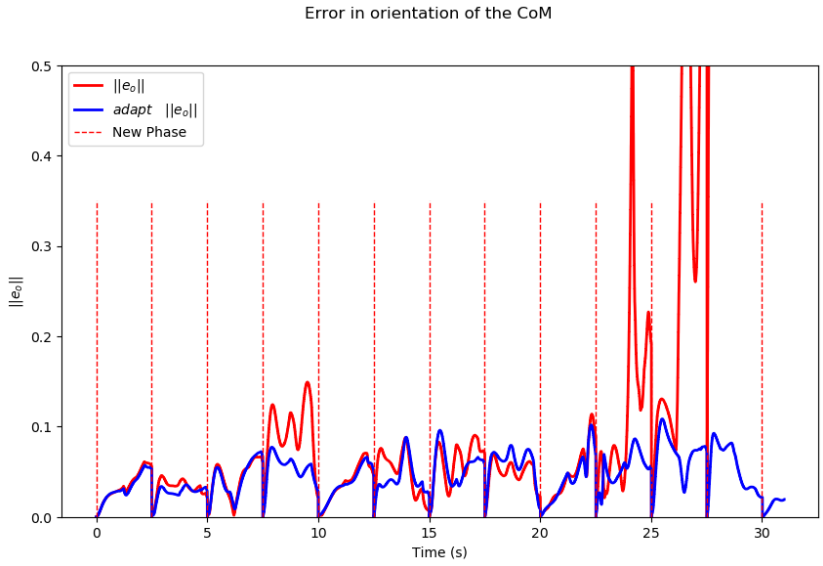

Figure 4.19: Error in orientation for the CoM, during adaptive forward locomotion.

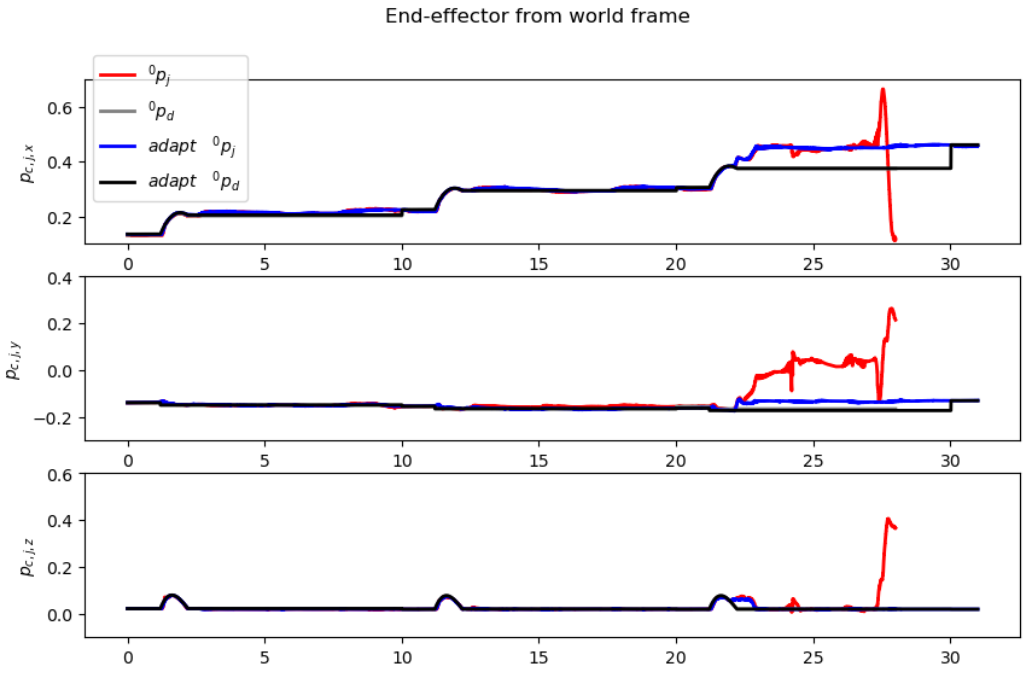

Figure 4.20: End-effector position of FR leg, with respect to 0 frame, during adaptive forward locomotion.

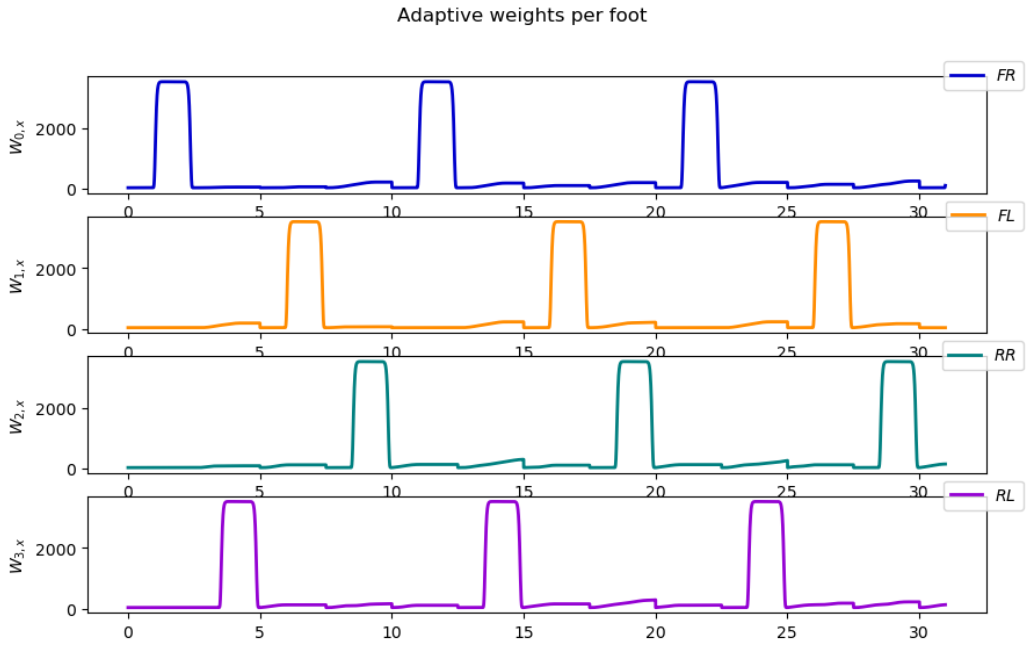

Figure 4.21: Adaptive weights of slip probability and super Gaussian adaptation for locomotion.

4.2.2 Conclusion

In this work, an adaptive trajectory tracking controller is proposed for quadruped robots, which involves two prioritized layers of adaptation for minimizing the slippage of one or multiple legs. The first adaptation layer considers the dynamic distribution of the control effort among the legs, given the slippage probability for each leg. The second layer, which is enabled only if the problem cannot be solved by the dynamic distribution of the effort, which may occur when all four legs slip, acts on the time-scaling of the trajectory by dynamically and smoothly slowing down the motion, without affecting the spatial properties of the task.

This approach has been established as asymptotically stable, guaranteeing the gradual convergence of the system to a stable state over time. Moreover, the combination of simulations and real-world experiments unequivocally demonstrates the method's capacity to enhance system robustness. It excels in minimizing leg slippage, consequently fostering both the stability and controllability of the robot.

In the context of the locomotion task, we observe that in the case of non-slippery terrains, the controller excels in tracking the desired position for the CoM, thereby ensuring stability. Furthermore, the consistent achievement of the desired CoM target in each instance ensures that the swinging leg precisely follows its intended path. This evidence underscores the "Body Movement" controller's effectiveness as a precise torque command controller, enabling agile movements, particularly in the context of locomotion.

Furthermore, when encountering terrain irregularities, such as slippery surfaces or even cylindrical objects on the ground, the suggested adaptive "Body Movement" controller demonstrates remarkable proficiency in overcoming these unforeseen circumstances. It has been observed that the robot lacking the adaptation mechanism does not have sufficient time to recover from such instances of slippage, resulting in a loss of control.

Overall, it is shown through simulations and experiments that the method equips the system with robustness, as it is able to minimize the slippage of the legs and it ensures the stability and controllability of the robot during agile manoeuvres and locomotion.

Chapter 5

Conclusions

Throughout this master's thesis we focused on enhancing the adaptivity of controllers when confronted with challenging terrains, particularly in scenarios involving slipping surfaces. Our objective encompassed the refinement of both trajectory tracking and reaching controllers to furnish them with the capability to swiftly adapt to external disturbances, especially during unmodeled contact events. The motivation behind this endeavor stems from our overarching goal of addressing the complex issues associated with agile maneuvers and locomotion across surfaces characterized by uncertain low-friction conditions, such as those defined by low-friction cones.

Building upon the foundation established in the preceding work, "Probabilistic Contact State" (referenced as [16]), we have undertaken the development and comprehensive exploration of diverse applications. These applications encompass a range of functions, including the optimization of body postures and the fine-tuning of body movements, with a central emphasis on harnessing the probabilistic information related to contact states. This approach extends our understanding of how probabilistic contact state data can be effectively leveraged across various aspects of our research and development endeavors.

In this research project, we introduce a novel set of adaptive trajectory tracking and locomotion controllers meticulously designed to address the unique challenges posed by quadruped robots navigating slippery terrains, with a particular emphasis on the innovative BPMC platform. These controllers represent a groundbreaking approach to enhance the robot's adaptability and performance, enabling it to traverse challenging environments with a heightened level of agility and precision.

The core objective of this work is to develop controllers that empower quadruped robots, such as those based on the BPMC, to navigate and operate effectively in conditions characterized by low friction, uneven surfaces, and potential slipping hazards. This is a critical endeavor, as it extends the capabilities of quadruped robots beyond controlled environments and into real-world scenarios where unpredictable terrains and conditions demand advanced locomotion strategies.

By proposing adaptive trajectory tracking and locomotion controllers, we are not

only advancing the state-of-the-art in robotics but also contributing to the field of autonomous navigation and mobility. These controllers are carefully engineered to optimize the robot's movement in slippery terrain, thus broadening the spectrum of potential applications, from search and rescue missions in challenging environments to the efficient exploration of complex terrains.

In more detail, the adaptive "Body Posture" controller, serving as the trajectory tracking controller, comprises two prioritized layers of adaptation aimed at minimizing slippage in one or multiple legs. The first adaptation layer takes into account the dynamic distribution of control effort among the legs, factoring in the slippage probability for each leg. The second layer, which becomes active when dynamic effort distribution alone cannot address the issue, intervenes by adjusting the time-scaling of the trajectory. This adjustment is executed in a dynamic and smooth manner, slowing down motion without affecting the spatial properties of the task.

Importantly, the proposed method demonstrates asymptotic stability. Simulations as well as real experiments validate its effectiveness in reducing leg slippage while ensuring the robot's stability and controllability. Notably, this is achieved without compromising the task space trajectory, a critical feature for applications in visual and depth-based Simultaneous Localization and Mapping. Stable and precise movement is paramount for the success of such approaches.

The "Body Movement" controller, serving as an adaptive reaching controller, plays a pivotal role in initiating locomotion tasks and executing agile maneuvers, particularly in challenging terrains marked by slipperiness and dynamic obstacles.

The core of the "Body Movement" controller lies in its initial layer, which ensures the equitable distribution of forces among all legs. Notably, this layer allows for the assignment of an exceptionally high weight to a specific leg, often designated as the swinging leg. This strategic assignment effectively excludes the swinging leg from the overall force distribution equation.

Throughout this process, the controller diligently maintains stability by accurately computing the center of the support polygon, aligning it with the CoM. This calculation takes into account only the legs in contact with the ground, commonly referred to as 'stance legs.' Significantly, the swinging leg remains uninvolved in the distribution of control effort, contributing to precise and stable locomotion.

On top of that, the "Body Movement" controller offers an additional layer that can be activated at the user's discretion, taking into account the probability of detecting slip events. This extra layer draws inspiration from the approach used in the first layer of the "Body Posture" controller. It dynamically adjusts the effort distribution among all legs based on the slip probability of each foot. This multifaceted approach not only introduces innovative concepts for agile movements but also ensures the stability of the robot's dynamic maneuvers. It represents a crucial step in advancing the adaptability and robustness of the overall system.

Furthermore, it is important to note that our approach avoids making the assumption that the surface in front of the robot consistently exhibits a uniform friction coefficient. In each new step, we re-evaluate the consideration of swing foot

weight, ensuring adaptability to varying surface conditions.

An adaptive locomotion controller of this nature is versatile and suitable for navigating through challenging terrains, be it indoor or outdoor environments. It offers enhanced adaptability and performance for a wide range of locomotion tasks.

Additionally, our research includes an extensive program of experimental evaluation, which has been conducted in a range of settings. We have meticulously tested our approach in both real-world and simulated scenarios, employing the GO1 quadruped robot as the primary test platform. This comprehensive assessment allowed us to gain valuable insights into the real-world applicability and performance of our method.

The outcomes of our experiments, derived from both simulated trials and real-world tests, underscore the effectiveness of our approach. We found that the method significantly enhances the system's robustness, making it capable of minimizing leg slippage. Moreover, it ensures the robot's stability and controllability, even in challenging conditions. This robustness and reliability represent significant milestones in advancing the capabilities of quadruped robots, making them better equipped to handle a wide array of real-world scenarios with precision and confidence.

In summary, our research represents a significant step forward in the realm of quadruped robot locomotion, introducing a set of adaptive controllers that promise to revolutionize the way these robots interact with and navigate slippery terrains, with the ultimate goal of making them more versatile, reliable, and robust in various real-world scenarios.

5.1 Future work

In our ongoing research endeavors we are actively exploring challenging, yet promising topics. A central aspect regards the generalization of terrains that are traversed by quadrupeds. In other words, we plan to extend our approach to the case of uneven and rough terrains characterized by varying inclinations. Our ultimate goal is to enhance both of the proposed controllers to accommodate the above mentioned terrains, utilizing as input 3D maps of the latter.

We are also actively exploring the integration of adaptive controllers with MPC. This collaborative approach aims to extend the temporal perspective, effectively lengthening the decision horizon for future steps in locomotion tasks. This strategic integration holds the potential to unlock a wide range of new possibilities, including the seamless incorporation of auxiliary tasks, such as pushing or carrying objects. The initiative, uniting the adaptability of our controllers with MPC, promises to significantly expand the spectrum of tasks and capabilities that our system can handle.

Another strand of our research involves the creation of a probability map that quantifies the risk associated with potential footholds. Our proposed approach leverages the power of machine learning, drawing insights from data acquired through depth cameras and 3D simulations. Our objective is to train a robust model

capable of distinguishing between secure footholds and those with a heightened risk probability. Through the amalgamation of depth data and simulations incorporating external forces, we aim to equip our robotic system with the capacity to identify secure and stable footholds, thus significantly enhancing navigation in challenging terrains and bolstering the overall safety of robotic locomotion tasks.

Lastly, we're in the process of refining our current approach for "Body Movement", specifically concerning the trajectories of swinging legs until they make contact with the ground. This refinement draws inspiration from related work developed for humanoid robots, as documented in [50].

Bibliography

[1] J. Tenreiro Machado and M. Silva, "An overview of legged robots," 04 2006.

[2] H. Taheri and N. Mozayani, "A study on quadruped mobile robots," *Mechanism and Machine Theory*, vol. 190, p. 105448, 2023. [Online]. Available: https://www.sciencedirect.com/science/article/pii/S0094114X23002197

[3] P. Biswal and P. K. Mohanty, "Development of quadruped walking robots: A review," *Ain Shams Engineering Journal*, vol. 12, no. 2, pp. 2017–2031, 2021. [Online]. Available: https://www.sciencedirect.com/science/article/pii/S2090447920302501

[4] C. Semini and P.-B. Wieber, "Legged Robots," in *Encyclopedia of Robotics*, M. H. Ang, O. Khatib, and B. Siciliano, Eds. Berlin, Heidelberg: Springer Berlin Heidelberg, 2020, pp. 1–8. [Online]. Available: http://link.springer.com/10.1007/978-3-642-41610-1_59-1

[5] K. Waldron and R. McGhee, "The adaptive suspension vehicle." *IEEE Control Systems Magazine*, pp. 7–12, 1986.

[6] *Holonomy and nonholonomy in the dynamics of articulated motion.* Proceedings of the Ruperto Carola Symposium on Fast Motion in Biomechanics and Robotics, 2005.

[7] M. Bjelonic, R. Grandia, O. Harley, C. Galliard, S. Zimmermann, and M. Hutter, "Whole-Body MPC and Online Gait Sequence Generation for Wheeled-Legged Robots," Jul. 2021, arXiv:2010.06322 [cs, eess]. [Online]. Available: http://arxiv.org/abs/2010.06322

[8] J. E. Bares and D. S. Wettergreen, "Dante ii: Technical description, results, and lessons learned," *The International Journal of Robotics Research*, vol. 18, no. 7, pp. 621–649, 1999. [Online]. Available: https://doi.org/10.1177/02783649922066475

[9] D. Bellicoso, M. Bjelonic, L. Wellhausen, K. Holtmann, F. Günther, M. Tranzatto, P. Fankhauser, and M. Hutter, "Advances in real-world applications for legged robots," *Journal of Field Robotics*, 10 2018.

[10] M. Tranzatto, T. Miki, M. Dharmadhikari, L. Bernreiter, M. Kulkarni, F. Mascarich, O. Andersson, S. Khattak, M. Hutter, R. Siegwart, and K. Alexis, "Cerberus in the darpa subterranean challenge," *Science Robotics*, vol. 7, 05 2022.

[11] J. Tenreiro Machado and M. Silva, "An overview of legged robots," in *International symposium on mathematical methods in engineering*, 2006, pp. 1–40.

[12] B. Aceituno-Cabezas, C. Mastalli, H. Dai, M. Focchi, A. Radulescu, D. G. Caldwell, J. Cappelletto, J. C. Grieco, G. Fernández-López, and C. Semini, "Simultaneous contact, gait, and motion planning for robust multilegged locomotion via mixed-integer convex optimization," *IEEE Robotics and Automation Letters*, vol. 3, no. 3, pp. 2531–2538, 2018.

[13] A. Hereid, C. M. Hubicki, E. A. Cousineau, and A. D. Ames, "Dynamic Humanoid Locomotion: A Scalable Formulation for HZD Gait Optimization," *IEEE Transactions on Robotics*, 2018.

[14] M. Vukobratović and B. Borovac, "ZERO-MOMENT POINT — THIRTY FIVE YEARS OF ITS LIFE," *International Journal of Humanoid Robotics*, vol. 01, no. 01, pp. 157–173, Mar. 2004. [Online]. Available: https://www.worldscientific.com/doi/abs/10.1142/S0219843604000083

[15] D.-E. Argiropoulos, "Maestro," https://github.com/despargy/maestro, 2023.

[16] M. Maravgakis, "Probabilistic contact estimation," https://github.com/MichaelMarav/ProbabilisticContactEstimation, 2022.

[17] D.-E. Argiropoulos, D. Papageorgiou, M. Maravgakis, D. Drosakis, and P. Trahanias, "Two-layer adaptive trajectory tracking controller for quadruped robots on slippery terrains," Apr. 2023, arXiv:2304.00804 [cs]. [Online]. Available: http://arxiv.org/abs/2304.00804

[18] D. Papageorgiou, D. E. Argiropoulos, and Z. Doulgeri, "Dirichlet-based dynamic movement primitives for encoding periodic motions with predefined accuracy," in *2022 31st IEEE International Conference on Robot and Human Interactive Communication (RO-MAN)*, 2022, pp. 1146–1152.

[19] F. Jenelten, J. Hwangbo, F. Tresoldi, C. D. Bellicoso, and M. Hutter, "Dynamic locomotion on slippery ground," *IEEE Robotics and Automation Letters*, vol. 4, no. 4, pp. 4170–4176, 2019.

[20] M. Camurri, M. Fallon, S. Bazeille, A. Radulescu, V. Barasuol, D. G. Caldwell, and C. Semini, "Probabilistic contact estimation and impact detection for state estimation of quadruped robots," *IEEE Robotics and Automation Letters*, vol. 2, no. 2, pp. 1023–1030, 2017.

[21] T.-Y. Lin, R. Zhang, J. Yu, and M. Ghaffari, "Legged robot state estimation using invariant kalman filtering and learned contact events," in *5th Annual Conference on Robot Learning*, 2021, p. [Online]].

[22] S. Piperakis, M. Maravgakis, D. Kanoulas, , and P. Trahanias, "Robust contact state estimation in humanoid walking gaits," in *IEEE/RSJ IROS*, 2022.

[23] M. Bloesch, M. Hutter, M. Hoepflinger, S. Leutenegger, C. D. R. C. Gehring, and R. Siegwart, "State estimation for legged robots: Consistent fusion of leg kinematics and imu," in *Proceedings of Robotics: Science and Systems, Sydney, Australia*, 2012.

[24] M. Bloesch, C. Gehring, P. Fankhauser, M. Hutter, M. A. Hoepflinger, and R. Siegwart, "State estimation for legged robots on unstable and slippery terrain," in *2013 IEEE/RSJ IROS*, 2013, pp. 6058–6064.

[25] J. Hwangbo, C. D. Bellicoso, P. Fankhauser, and M. Hutter, "Probabilistic foot contact estimation by fusing information from dynamics and differential/forward kinematics," in *2016 IEEE/RSJ IROS*, 2016, pp. 3872–3878.

[26] Z. Fu, A. Kumar, A. Agarwal, H. Qi, J. Malik, and D. Pathak, "Coupling Vision and Proprioception for Navigation of Legged Robots," Jul. 2022, arXiv:2112.02094 [cs]. [Online]. Available: http://arxiv.org/abs/2112.02094

[27] F. Jenelten, T. Miki, A. E. Vijayan, M. Bjelonic, and M. Hutter, "Perceptive locomotion in rough terrain – online foothold optimization," *IEEE Robotics and Automation Letters*, vol. 5, no. 4, pp. 5370–5376, 2020.

[28] P. Fankhauser, M. Bjelonic, C. Dario Bellicoso, T. Miki, and M. Hutter, "Robust rough-terrain locomotion with a quadrupedal robot," pp. 5761–5768, 2018.

[29] F. Jenelten, R. Grandia, F. Farshidian, and M. Hutter, "Tamols: Terrain-aware motion optimization for legged systems," *IEEE Transactions on Robotics*, vol. 38, no. 6, pp. 3395–3413, 2022.

[30] M. Focchi, V. Barasuol, M. Frigerio, D. Caldwell, and C. Semini, "Slip detection and recovery for quadruped robots," 09 2015.

[31] G. Xin, W. Wolfslag, H.-C. Lin, C. Tiseo, and M. Mistry, "An optimization-based locomotion controller for quadruped robots leveraging cartesian impedance control," *Frontiers in Robotics and AI*, vol. 7, 03 2020.

[32] C. Gehring, C. Dario Bellicoso, P. Fankhauser, S. Coros, and M. Hutter, "Quadrupedal locomotion using trajectory optimization and hierarchical whole body control," in *2017 IEEE International Conference on Robotics and Automation (ICRA)*, 2017, pp. 4788–4794.

[33] S. Fahmi, C. Mastalli, M. Focchi, and C. Semini, "Passive Whole-body Control for Quadruped Robots: Experimental Validation over Challenging Terrain," Mar. 2019, arXiv:1811.00884 [cs]. [Online]. Available: http://arxiv.org/abs/1811.00884

[34] T. Miki, J. Lee, J. Hwangbo, L. Wellhausen, V. Koltun, and M. Hutter, "Learning robust perceptive locomotion for quadrupedal robots in the wild," *Science Robotics*, vol. 7, no. 62, 1 2022. [Online]. Available: https://doi.org/10.1126%2Fscirobotics.abk2822

[35] D. Hoeller, N. Rudin, C. Choy, A. Anandkumar, and M. Hutter, "Neural scene representation for locomotion on structured terrain," 2022. [Online]. Available: https://arxiv.org/abs/2206.08077

[36] O. Villarreal, V. Barasuol, M. Camurri, L. Franceschi, M. Focchi, M. Pontil, D. G. Caldwell, and C. Semini, "Fast and Continuous Foothold Adaptation for Dynamic Locomotion through CNNs," *IEEE Robotics and Automation Letters*, vol. 4, no. 2, pp. 2140–2147, Apr. 2019, arXiv:1809.09759 [cs]. [Online]. Available: http://arxiv.org/abs/1809.09759

[37] T. Horvat, K. Melo, and A. J. Ijspeert, "Model predictive control based framework for com control of a quadruped robot," in *2017 IEEE/RSJ International Conference on Intelligent Robots and Systems (IROS)*, 2017, pp. 3372–3378.

[38] S. Xu, L. Zhu, and C. P. Ho, "Learning efficient and robust multi-modal quadruped locomotion: A hierarchical approach," in *2022 International Conference on Robotics and Automation (ICRA)*, 2022, pp. 4649–4655.

[39] Y. You, Z. Yang, T. Zou, Y. Sui, C. Xu, C. Zhang, H. Xu, Z. Zhang, and J. Han, "A new trajectory tracking control method for fully electrically driven quadruped robot," *Machines*, vol. 10, p. 292, 04 2022.

[40] Z. Li, X. Chen, X. Peng, D. Fan, and D. Xu, "A trajectory tracking control method for quadruped robot based on limit value," in *2021 China Automation Congress (CAC)*, 2021, pp. 3068–3073.

[41] R. Khusainov, A. Klimchik, and E. Magid, "Swing Leg Trajectory Optimization for a Humanoid Robot Locomotion:," in *Proceedings of the 13th International Conference on Informatics in Control, Automation and Robotics*. Lisbon, Portugal: SCITEPRESS - Science and and Technology Publications, 2016, pp. 130–141. [Online]. Available: http://www.scitepress.org/DigitalLibrary/Link.aspx?doi=10.5220/0006011401300141

[42] D. T. De Paula, E. Paciencia Godoy, and M. Becerra-Vargas, "Towards Dynamic Quadruped Locomotion: Development of a CPG-driven Foot Trajectory Generator," in *2022 30th Mediterranean Conference on Control and Automation (MED)*. Vouliagmeni, Greece: IEEE, Jun. 2022, pp. 988–993. [Online]. Available: https://ieeexplore.ieee.org/document/9837290/

[43] M. Haberland, J. D. Karssen, S. Kim, and M. Wisse, "The effect of swing leg retraction on running energy efficiency," in *2011 IEEE/RSJ International Conference on Intelligent Robots and Systems*, 2011, pp. 3957–3962.

[44] M. Maravgakis, D.-E. Argiropoulos, S. Piperakis, and P. Trahanias, "Probabilistic contact state estimation for legged robots using inertial information," in *2023 IEEE International Conference on Robotics and Automation (ICRA)*, 2023, pp. 12 163–12 169.

[45] P. G. de Santos, E. Garcia, and J. Estremera, *Quadrupedal Locomotion: An Introduction to the Control of Four-legged Robots*. Springer London, 2006, ch. Stability Measurements.

[46] A. J. Ijspeert, J. Nakanishi, H. Hoffmann, P. Pastor, and S. Schaal, "Dynamical movement primitives: Learning attractor models for motor behaviors," *Neural Comput.*, vol. 25, no. 2, pp. 328–373, Feb 2013.

[47] L. Alacoque and K. James, "Topology optimization with variable loads and supports using a super-gaussian projection function," *Structural and Multidisciplinary Optimization*, vol. 65, 02 2022.

[48] S. Baydas and B. Karakas, "Defining a curve as a bezier curve," *Journal of Taibah University for Science*, vol. 13, pp. 522–528, 12 2019.

[49] P. E. Bézier and S. Sioussiou, "Semi-automatic system for defining free-form curves and surfaces," *Computer-Aided Design*, vol. 15, no. 2, pp. 65–72, 1983. [Online]. Available: https://www.sciencedirect.com/science/article/pii/0010448583901707

[50] A. A. Saputra, A. S. Khalilullah, I. A. Sulistijono, and N. Kubota, "Adaptive motion pattern generation on balancing of humanoid robot movement," in *2015 IEEE 28th Canadian Conference on Electrical and Computer Engineering (CCECE)*, 2015, pp. 1479–1484.

[51] L. Koutras and Z. Doulgeri, "Exponential stability of trajectory tracking control in the orientation space utilizing unit quaternions," in *2021 IEEE/RSJ IROS*, 2021, pp. 8151–8158.

Appendix

Global asymptotic stability (3.10)

After substituting (3.10) in (3.5), we get the following closed loop system dynamics:

$$\mathbf{H}_c\dot{\mathbf{e}}_v = -(\mathbf{C}_c + \mathbf{K}_v)\mathbf{e}_v - \begin{bmatrix} k_p\mathbf{e}_p \\ k_o\mathbf{e}_o \end{bmatrix}, \tag{5.1}$$

$$\begin{bmatrix} \dot{\mathbf{e}}_p \\ \dot{\mathbf{e}}_o \end{bmatrix} = \begin{bmatrix} \mathbf{I}_3 & \mathbf{0}_3 \\ \mathbf{0}_3 & \mathbf{J}_l(\mathbf{e}_o) \end{bmatrix} \mathbf{e}_v, \tag{5.2}$$

where $\mathbf{J}_l(\mathbf{e}_o) \in \mathbb{R}^{3\times3}$ the matrix mapping the orientation part of $\mathbf{e}_v$ to $\dot{\mathbf{e}}_o$, as detailed in [51], for which the following holds: $\mathbf{J}_l^\intercal\mathbf{e}_o = \mathbf{J}_l\mathbf{e}_o = \mathbf{e}_o$ (as shown in [51]).

Theorem 1. *The origin of the state-space of the system (5.1), i.e.* $(\mathbf{e}_p, \mathbf{e}_o, \mathbf{e}_v) = (\mathbf{0}, \mathbf{0}, \mathbf{0})$*, is globally asymptotically stable.*

Proof. Consider the following candidate Lyapunov function:

$$L = \frac{k_p}{2}|\mathbf{e}_p|^2 + \frac{k_o}{2}|\mathbf{e}_o|^2 + \frac{1}{2}\mathbf{e}_v^\intercal\mathbf{H}_c\mathbf{e}_v. \tag{5.3}$$

By taking its time derivative, we get $\dot{L} = k_p\mathbf{e}_p^\intercal\dot{\mathbf{e}}_p + k_o\mathbf{e}_o^\intercal\dot{\mathbf{e}}_o + \frac{1}{2}\mathbf{e}_v^\intercal\dot{\mathbf{H}}_c\mathbf{e}_v + \mathbf{e}_v^\intercal\mathbf{H}_c\dot{\mathbf{e}}_v$. After substituting $\mathbf{H}_c\dot{\mathbf{e}}_v$ from (5.1) and utilizing the skew symmetric property, i.e. $\mathbf{e}_v^\intercal\left(\dot{\mathbf{H}}_c - 2\mathbf{C}_c\right)\mathbf{e}_v = 0$, we get:

$$\dot{L} = k_p\mathbf{e}_p^\intercal\dot{\mathbf{e}}_p + k_o\mathbf{e}_o^\intercal\dot{\mathbf{e}}_o + \mathbf{e}_v^\intercal\left(-\mathbf{K}_v\mathbf{e}_v - \begin{bmatrix} k_p\mathbf{e}_p \\ k_o\mathbf{e}_o \end{bmatrix}\right). \tag{5.4}$$

By utilizing (5.2) and the property $\mathbf{J}_l^\intercal\mathbf{e}_o = \mathbf{J}_l\mathbf{e}_o = \mathbf{e}_o$, (5.4) becomes: $\dot{L} = -\mathbf{K}_v\mathbf{e}_v^\intercal\mathbf{e}_v$,which is less or equal to zero for all $\mathbf{e}_p \neq \mathbf{0}, \mathbf{e}_o \neq \mathbf{0}, \mathbf{e}_v \neq \mathbf{0}$. Hence, by invoking the LaSalle theorem we can conclude that the origin is globally asymptotically stable. □